Investigating fibrosis and inflammation in an ex vivo NASH murine model

Gore, Emilia; Bigaeva, Emilia; Oldenburger, Anouk; Jansen, Yvette J M; Schuppan, Detlef; Boersema, Miriam; Rippmann, Joerg F; Broermann, Andre; Olinga, Peter

Published in:
American Journal of Physiology. Gastrointestinal and Liver Physiology

DOI:
10.1152/ajpgi.00209.2019

Publication date:
2020

Investigating fibrosis and inflammation in an *ex vivo* NASH murine model

Emilia Gore[1], Emilia Bigaeva[1], Anouk Oldenburger[2], Yvette J. M. Jansen[1], Detlef Schuppan[3, 4], Miriam Boersema[1], Jörg F. Rippmann[2], Andre Broermann[2] and Peter Olinga[1#]

[1]Pharmaceutical Technology and Biopharmacy, University of Groningen, Groningen, The Netherlands

[2]CardioMetabolic Diseases Research, Boehringer Ingelheim Pharma GmbH & Co. KG, Biberach an der Riss, Germany

[3]Institute of Translational Immunology and Research Center for Immunotherapy, University Medical Center, Johannes Gutenberg University, Mainz, Germany

[4]Division of Gastroenterology, Beth Israel Deaconess Medical Center, Harvard Medical School, Boston, MA, USA

Running head: Investigating an *ex vivo* NASH model

[#]Correspondence to:

Prof P. Olinga

University of Groningen, Department of Pharmaceutical Technology and Biopharmacy,

Antonius Deusinglaan 1, 9713AV Groningen, the Netherlands

Tel: +3150-3638373

E-mail: p.olinga@rug.nl

Orcid number:

Emilia Gore (0000-0001-5553-186X)

Emilia Bigaeva (0000-0002-8903-4025)

Anouk Oldenburger (0000-0002-0264-2467)

Yvette J.M. Jansen (0000-0002-2847-8116)

Detlef Schuppan (0000-0002-4972-1293)

Miriam Boersema (0000-0001-9356-796X)

Jörg F. Rippmann (0000-0002-6666-6222)

Andre Broermann (0000-0002-4768-9074)

Peter Olinga (0000-0003-4855-8452)

Abstract

Nonalcoholic fatty liver disease (NAFLD) is the most common liver disease, characterized by excess fat accumulation (steatosis). Nonalcoholic steatohepatitis (NASH) develops in 15-20% of NAFLD patients, and frequently progresses to liver fibrosis and cirrhosis. We aimed to develop an *ex vivo* model of inflammation and fibrosis in steatotic murine precision-cut liver slices (PCLS). NASH was induced in C57Bl/6 mice using amylin and choline-deficient L-amino acid-defined (CDAA) diet. PCLS were prepared from steatohepatitic (sPCLS) and control (cPCLS) livers and cultured for 48h with LPS, TGFβ1 or elafibranor. Additionally, C57Bl/6 mice were placed on CDAA diet for 12 weeks, to receive elafibranor or vehicle from week 7-12. Effects were assessed by transcriptome analysis and pro-collagen Iα1 protein production. The diets induced features of human NASH. Upon culture, all PCLS showed an increased gene expression of fibrosis and inflammation related markers, but decreased lipid metabolism markers. LPS and TGFβ1 affected sPCLS more pronouncedly than cPCLS. TGFβ1 increased pro-collagen Iα1 solely in cPCLS. Elafibranor ameliorated fibrosis and inflammation *in vivo*, but not *ex vivo*, where it only increased the expression of genes modulated by PPARα. sPCLS culture induced inflammation, fibrosis and lipid metabolism related transcripts, explained by spontaneous activation. sPCLS remained responsive to pro-inflammatory and profibrotic stimuli on gene expression. We consider that PCLS represent a useful tool to reproducibly study NASH progression. sPCLS can be used to evaluate potential treatments for NASH, as demonstrated in our elafibranor study, and serves as a model to bridge results from rodent studies to the human system.

Keywords: NASH, precision-cut liver slices, inflammation, fibrosis, elafibranor

68 **New & Noteworthy**

69 This study showed that nonalcoholic steatohepatitis can be studied *ex vivo* in precision-cut
70 liver slices obtained from murine diet-induced fatty livers.

71 Liver slices develop a spontaneous inflammatory and fibrogenic response during culture that
72 can be augmented with specific modulators. Additionally, the model can be used to test the
73 efficacy of pharmaceutical compounds (as shown in this investigation with elafibranor) and
74 could be a tool for preclinical assessment of potential therapies.

75

Introduction

Nonalcoholic fatty liver disease (NAFLD) is the main cause of chronic liver disease in Europe and USA(71), with increasing prevalence. The pathogenesis of NAFLD is not completely understood; however, the genetic predisposition, obesity, type 2 diabetes mellitus, hyperlipidemia and the metabolic syndrome are closely associated(24, 71). NAFLD includes benign steatosis (fat accumulation) and nonalcoholic steatohepatitis (NASH), which is characterized by ballooning degeneration and lobular inflammation that can lead to fibrosis, cirrhosis and hepatocellular carcinoma(47).

Currently there are no approved pharmacological therapies to treat NASH. Lifestyle interventions (e.g. weight loss and exercise) are recommended by the American Association for the Study of Liver Disease(7), but due to lack of compliance, these cannot be implemented in the majority of patients. Most drugs in clinical trials that target NASH address upstream mechanisms related to hepatic steatosis and metabolic stress(45).

To advance the scientific understanding of NAFLD and NASH, and to test novel drug candidates, adequate animal models are essential. The perfect animal model represents the plethora of pathophysiological changes observed in patients. Conventional mouse models are based on *ad libitum* feeding of diets enriched in different combinations of fat, fructose, cholesterol, nutrient deficiencies (e.g., choline and/or methionine), toxic interventions or genetic manipulation(29). Overnutrition in rodents shows satisfactory results and similarities to the human pathology of mere obesity and type 2 diabetes(8, 27), although the phenotype is typically mild NASH with no or minimal fibrosis. Thus, there is a clear need for preclinical models that reproduce both the disease phenotype and its etiology, to support the mechanistic and pharmacological studies of NASH in man(13).

The amylin liver NASH model (AMLN) is overnutrition-based by incorporates food pellets that combine fat (≈40%) with fructose (≈20%), a monosaccharide promoting NAFLD severity(32). This leads to macro- and microvesicular steatosis, periportal inflammation, portal and bridging fibrosis after 30 weeks(10). Another option for inducing NASH is a nutrient deficient diet. The best such model is the choline-deficient L-amino acid-defined (CDAA)

diet(13) that causes NASH due to the absence of choline, an essential nutrient, needed for triglyceride packaging and export as very low density lipoprotein, and bile salt excretion from hepatocytes(30, 38). Mice fed with this diet develop steatosis, inflammation and fibrosis(25). However, the grade of inflammation and fibrosis can be variable, depending on the mouse strain and other food components(21).

To improve reproducibility of NASH-related inflammation and fibrosis, to permit a standardized test model for potential drugs, such as anti-inflammatory or antifibrotic agents, and to save on experimental animals, we studied the validity of *ex vivo* murine model of precision-cut liver slices (PCLS). PCLS preserve the complex structure of the liver and its cellular interactions, showing a spontaneous profibrotic and pro-inflammatory response during culture(33, 67). Inflammation and fibrosis can be further enhanced by incubating PCLS with TGFβ1 and LPS, respectively(54, 56). Of note, TGFβ1 and LPS are also involved in NAFLD pathology and progression(17, 65). Last, PCLS is a valuable preclinical tool that allows drug testing for efficacy and toxicity(33, 61), while considerably reducing the number of experimental animals. For instance, Ijssennagger et al. successfully tested the effect of obeticholic acid (drug in phase III clinical trials for NASH) in PCLS, providing new insights into the mechanism of action(22).

In this study, we aimed to develop and standardize an *ex vivo* model based on steatotic PCLS obtained from livers of mice subjected to two diets that induce NASH, namely AMLN and CDAA diets.

Methods

Chemicals

LPS was purchased at SAS Invivogen (TLRL-3PELPS, Toulouse, France) and human recombinant TGFβ1 was purchased from R&D Systems (240-B-002, Abingdon, UK). They were reconstituted according to the provider's instructions. Elafibranor was purchased from (Sage Chemicals, Johannesburg, South Africa) and dissolved in DMSO. All stocks were stored at -20°C.

Animals for *ex vivo* studies

Adult male C57Bl/6JRj (Bl/6) mice from Janvier were placed on a Choline Deficient L-Amino Acid (CDAA, E15666-94, Ssniff Spezialdiäten GmbH) diet for 12 weeks (10 animals on CDAA diet and 8 on control diet) or amylin liver NASH model diet (AMLN, D09100301, Research Diets, NJ, USA) for 26 weeks (4 animals on AMLN diet and 4 on control diet). Each NAFLD-inducing diet had its matching control diet. The mice were housed on a 12h light/dark cycle, with controlled temperature and humidity. Chow and drinking water were *ad libitum*. The mice were sacrificed under isoflurane/O_2 (Nicholas Piramal, London, UK) anesthesia. The studies were approved by the Animal Review Committee of the German government and were performed according to the German Animal Protection Law.

Animals for *in vivo* studies

Male 8-week-old Bl/6 mice from Janvier were placed on CDAA. After 6 weeks of diet, the animals were treated with 15 mg/kg elafibranor (administered orally twice a day) or vehicle for 6 weeks, while continuing the diet (11 mice in each group). The studies were approved by the Animal Review Committee of the German government and were performed according to the German Animal Protection Law.

Preparation of precision-cut liver slices

We excised the mouse livers and collected them in ice-cold University of Wisconsin preservation solution (DuPont Critical Care, Waukegab, IL, USA). The tissue was kept on ice until preparation of PCLS.

PCLS were prepared as previously described(18) from the whole liver, with a Krumdieck tissue slicer (Alabama Research and Development, USA). PCLS had the following characteristics: diameter – 5 mm, thickness – 250-300 μm, weight – 4-5 mg. We incubated the PCLS individually in 12-well plates in 1.3 ml of Williams Medium E (with L glutamine, Invitrogen, Paisly, Scotland) supplemented with 25 mM glucose and 50 μg/ml gentamycin (Invitrogen). PCLS were exposed to 1 μg/ml LPS, 5 ng/ml TFGβ or elafibranor 0.2 or 1 μM. Culture medium was changed after 24h. Culture lasted 48h. PCLS were cultured in an incubator (Binder, Tuttlingen, Germany) with 37°C, 90% O_2 and 5% CO_2, horizontally shaken at 90 rpm. An outline of the sample preparation is presented in Fig. 1.

PCLS viability

PCLS viability was assessed by adenosine triphosphate (ATP) content with a bioluminescence kit (Roche Diagnostics, Mannheim, Germany). The obtained ATP content (pmol) was corrected for the total protein content (μg), determined with the Lowry method (RC DC Protein Assay, Bio Rad, Veenendaal, The Netherlands).

Gene expression analysis

We used quantitative reverse transcription polymerase chain reaction (qRT-PCR) as a method to evaluate the gene expression of markers related to fibrosis, inflammation and fat metabolism. Three PCLS were pooled, snap-frozen and RNA was extracted with FavorPrep™ Tissue Total RNA Mini Kit (Favorgen, Vienna, Austria). We determined RNA quantity and quality with BioTek Synergy HT (BioTek Instruments, Vermont, USA). 1 μg total RNA was reverse transcribed to cDNA using the Reverse Transcription System (Promega, Leiden, The Netherlands). qRT-PCR was performed using ViiA 7 Real-Time PCR System (Applied Biosystems, California, USA) and SYBR Green (Roche) based detection. We assessed the gene expression of the selected markers (Supplementary Information Table 1) with the Double Delta Ct analysis ($2^{-\Delta\Delta Ct}$), using Hydroxymethylbilane Synthase (*Hmbs*) as a reference gene.

Hydroxyproline analysis

Hepatic hydroxyproline (hyp) was determined from 250-350 mg tissue, which was hydrolyzed in 5 ml of HCl 6N overnight at 110°C. The samples were diluted in citric-acetate buffer and

treated with Chloramine T (Sigma-Aldrich, Zwijndrecht, Netherlands) and 4-(dimethyl)aminobenzaldehyde (Sigma-Aldrich). The absorbance of the samples was measured at 550 nm. The results show the µg of hepatic hyp per mg tissue.

Histopathological analysis

Formalin-fixed, paraffin embedded PCLS were sectioned at 4 µm and stained with hematoxylin and eosin (H&E) to assess hepatic steatosis, sirius red (SR) and Masson's trichrome for collagen deposition. The images were acquired with NanoZoomer S360 (Hamamatsu, Hamamatsu, Japan) and the quantification of the SR staining was performed using the Aperio ImageScope software (Leica Biosystems, IL, USA).

Serum triglyceride

Serum triglyceride content was assessed in a COBAS Integra 400 plus (Roche Diagnostics, Mannheim, Germany) using the provided protocol.

Pro-collagen Iα1

We measured the content of murine pro-collagen Iα1 in the culture media of PCLS using an ELISA kit (ab210579, Cambridge, UK). The determination was performed on media from the last 24h of culture and pooled from three slices of the same group. The assay was done according to the manufacturer's protocol.

Data and statistical analysis

We used 4 to 10 different livers per diet, using slices in triplicates from each liver. The results are presented as mean ± standard error of the mean (SEM). Significance was established using non-parametric tests: Mann-Whitney test (unpaired and two-tailed p value) when comparing two groups and Kruskal-Wallis test (exact p value) when comparing three groups. The difference was considered significant when $p<0.05$.

Results

AMLN and CDAA diets induce NASH-associated changes

We initially evaluated the presence of liver steatosis and fibrosis. To this end, we assessed the differences in liver to body weight (LBW) ratio, hydroxyproline (hyp) content, histology and transcriptional levels of fibrosis, inflammation and fat metabolism markers (Fig. 2). First, the LBW ratio (Fig. 2A) showed a marked difference between the NASH diets and their controls, indicating liver enlargement mainly due to steatosis. Second, the hyp content (Fig. 2B) revealed the presence of fibrosis in AMLN and CDAA livers, where the concentration of hyp/mg liver increased by 100% and 500%, respectively. Third, the morphological analysis showed that the NASH diets led to liver steatosis, characterized by macrovesicular steatosis in CDAA-fed mice and macro- and microvesicular steatosis in AMLN fed animals (Fig. 2C). Additionally, we observed infiltrating immune cells in sections from both diets. The Sirius Red (Fig. 2C) and Masson's trichrome (SI Fig. 1) stainings revealed the presence of fibrosis in both models, with the mice on the CDAA diet having more ECM deposition. Last, we investigated the differences in gene expression of several markers related to fibrosis, inflammation and fat metabolism in PCLS prior culture (Fig. 2D). Fibrosis markers (*Col1α1, Serpinh1, Acta2*) were increased in the diets compared to control. *Fn1* showed an increase only for the CDAA diet. We next evaluated inflammation by measuring gene transcription of cytokines: IL-1b, IL-6 and TNFα. Increased gene expression of *Il1b* and *Tnfa* was observed for both diets. To assess the transcriptional changes associated with fat metabolism, we tested the gene expression of two anabolism markers involved in fatty acid synthesis (*Fasn*, *Acaca*) and three markers related to fatty acid catabolism (*Acox*, *Cpt1a*, *Ppara*). All tested lipid metabolism markers were downregulated by the CDAA diet, while no difference was observed for the AMLN diet. These PCR results were obtained by comparing each NAFLD diet to its respective control diet; however, there were certain differences at baseline between the two control diets (SI Fig. 2), which are not the focus of this study and were not taken into consideration for the next

analyses. These results show major diet-induced changes related to hepatic fat accumulation, fibrosis and inflammation, which mimic pathological characteristics of human NASH.

Culture of steatotic PCLS induces fibrosis and inflammation and reduces fat metabolism

Tissue slicing and culture induces a pro-inflammatory and profibrotic response, most probably due to the mechanical stress and cold ischemia(33, 55, 66). Therefore, we assessed the effect of culture on all PCLS. Slices maintained viability during the 48h of culture (SI Fig. 3A). Next, we analyzed transcriptional changes for fibrosis, inflammation and fat metabolism related markers. To facilitate comparison, we divided the slices into two groups: steatotic PCLS – sPCLS (from the livers of mice on AMLN and CDAA diets) and control PCLS – cPCLS from the corresponding control diets.

PCLS culture increased gene expression of fibrosis markers (*Col1a1*, *Serpinh1* and *Fn1*) in all groups (Fig. 3A). Moreover, the expression levels reached in sPCLS were higher than cPCLS. We also observed that the gene expression levels of these three markers were higher in sPCLS from mice livers of CDAA than AMLN. The expression of the myofibroblast activation marker *Acta2* was increased only in sPCLS. The results show that incubation triggers a profibrotic response in healthy and steatotic PCLS.

Next, the inflammation status was evaluated through the gene expression of *Il1b*, *Il6* and *Tnfa* (Fig. 3B). Culture-induced changes for *Il1b* were represented by a small gene expression increase in AMLN cPCLS. The gene expression of *Il6* was strongly upregulated during incubation and we observed differences between sPCLS (100-200 times fold induction compared to cPCLS prior incubation) and cPCLS (30-40 times fold induction). Similarly, *Tnfa* gene expression was increased in all groups, with sPCLS reaching a higher expression level than their corresponding cPCLS. Altogether, this shows that the presence of steatosis in PCLS has a synergistic effect on the induction of transcripts of inflammation during culture.

Further, we evaluated transcriptional changes related to lipid anabolism by measuring the expression of *Fasn* and *Acaca* (Fig. 3C). Culture decreased the expression of *Fasn* in all groups except CDAA sPCLS. Similarly, *Acaca* was downregulated in AMLN sPCLS and

CDAA cPCLS. Of note, the expression levels of *Fasn* and *Acaca* in CDAA sPCLS compared to CDAA cPCLS were already decreased prior to the culture. Regarding the transcription of lipid catabolism markers (Fig. 3C), culture led to a decrease in the gene expression of *Acox*, *Cpt1a* and *Ppara* in most of the groups. Thus, culture of steatotic and control PCLS for 48h reduces the gene expression of lipid metabolism related markers.

Fibrosis and inflammation can be further enhanced in PCLS with activating mediators

LPS is a bacterial endotoxin that generates an immune response characterized by the induction of proinflammatory cytokines(62). TGFβ1 is a multifunctional cytokine and is one of the main promoters of fibrosis(37). Both molecules are extensively used in *in vitro* research, due to their well-characterized and reproducible responses. We treated the PCLS with LPS or TGFβ1 for 48h to assess if inflammation and fibrosis could be further enhanced. All PCLS remained viable during culture (SI Fig. 3B), but TGFβ1 reduced the ATP content by 20% in AMLN cPCLS and CDAA sPCLS. No significant differences were observed between the fibrotic areas of AMLN, CDAA s/cPCLS treated with TGFβ1 and untreated PCLS (SI Fig. 4).

Next, we analyzed LPS and TGFβ1 induced gene expression changes. LPS had almost no effect on the expression of fibrosis markers (Fig. 4A), with the exception of a small increase in *Serpinh1* and *Acta2* expression in AMLN sPCLS. Additionally, no effect was observed on the content of pro-collagen Iα1 released in culture media (Fig. 4B). As expected, the main effect of LPS was observed in the expression of inflammation markers (Fig. 4C). In all groups (except *Il1b* in CDAA cPCLS), LPS increased the gene expression of inflammatory markers. Moreover, in both diets, the treatment with LPS led to a higher gene expression level of *Il1b*, *Il6* and *Tnfa* in sPCLS than cPCLS. With regard to lipid metabolism markers (Fig. 4D), LPS reduced exclusively the expression of catabolism markers: *Acox* (AMLN sPCLS), *Cpt1a* (AMLN sPCLS) and *Ppara* (AMLN c/sPCLS and CDAA cPCLS). These results show that LPS induces an additional inflammatory effect and can also affect lipid catabolism.

In all groups, TGFβ1 increased the gene expression of all studied fibrosis markers (Fig. 5A), except AMLN cPCLS, which showed an increase, but was not statistically significant. After

TGFβ1 treatment, the gene expression level of sPCLS was higher than in cPCLS (for *Col1α1*, *Acta2*, *Serpinh1*). With regards to the secretion of pro-collagen Iα1, TGFβ1 increased the production of this protein solely in the control diets (Fig. 5B). Beside fibrosis, TGFβ1 also influenced transcripts of inflammation (Fig. 5C) and lipid metabolism in certain groups (Fig. 5D). Hence, PCLS treated with TGFβ1 displayed transcriptional changes related to fibrosis (increase), inflammation (slight increase) and lipid metabolism (decrease), especially in the presence of steatosis.

PPARα/δ agonist increases lipid metabolism in the *ex vivo* CDAA model

Elafibranor, a PPARα/δ agonist, is a potential treatment for NASH, which is now investigated in a phase 3 clinical trial (https://clinicaltrials.gov/ct2/show/NCT02704403). Our *ex vivo* NASH model has the potential of becoming a drug-testing system that can help evaluate the efficacy of drugs to reduce steatosis, inflammation and/or fibrosis. A critical validation step for this *ex vivo* model is to provide evidence of target engagement and pharmacological effects of the drugs that have been proven effective in *in vivo* studies. Therefore, we investigated the effect of elafibranor in PCLS from CDAA-induced NASH. We selected the CDAA model due to the higher amount of hepatic fibrosis compared to AMLN model and the possibility of direct comparison to *in vivo* results(63). We tested two concentrations of elafibranor, 0.2 μM and 1 μM, based on the half maximal effective concentration of the drug(31). Elafibranor was well tolerated in PCLS, and a decrease in ATP content (25%) was observed only in cPCLS when treated with the 1 μM concentration (SI Fig. 3C). After 48h treatment, there were no changes regarding the gene expression of fibrosis and inflammation markers and pro-collagen Iα1 production in PCLS treated with elafibranor compared to untreated PCLS of the same diet (Fig. 6A, B, C).

Treatment of PCLS with elafibranor had no effect on the gene expression of fat anabolism markers, *Acaca* and *Fasn* (Fig. 6D). Regarding fat catabolism, the gene expression of *Acox* was increased by elafibranor 1 μM in sPCLS; additionally, we observed a trend of increased gene expression for *Acox* and *Ppara* in cPCLS. Considering that the increased expression of *Acox* is a direct effect of PPARα stimulation(43), we further tested several other markers that

314 are regulated by PPARα/δ in mice(3, 11, 36, 42, 43). These include genes involved in: fatty
315 acid oxidation and ketogenesis (*Cyp4a*, *Acadm*, *Hmgcs2*), fatty acid transport (*Cd36*, *Fabp1*),
316 production of fatty acids and very low density lipoproteins (*Me1*, *Scd1*), apolipoproteins
317 (*Apoa2*, *Apoa5*), triglyceride clearance (*Angptl4*), glucose metabolism (*Pdk4*) and peroxisome
318 proliferation (*Pex11a*). The differences regarding these genes between CDAA diet and its
319 control, prior incubation, are presented in SI Fig. 5. After 12 weeks of diet, the gene expression
320 of *Fabp1*, *Scd1*, *Me1*, *Apoa5* and *Pex11a* were significantly decreased compared to control
321 diet. Moreover, a trend for decreased gene expression is observed for *Cyp4a* (p=0.06) and
322 *Apoa2* (p=0.06). The effects of elafibranor on these genes in PCLS are presented in Fig. 6D.
323 Elafibranor 1 μM increased the gene expression of *Cyp4a* in both cPCLS and sPCLS. The
324 sPCLS responded more pronouncedly than the cPCLS; moreover, sPCLS treated with
325 elafibranor 1 μM showed a gene expression level that was 2-fold higher than cPCLS at 0h.
326 Elafibranor increased in PCLS the gene expression of enzymes involved in microsomal
327 (*Cyp4a*) and peroxisomal (*Acox*) fatty acid oxidation, but not mitochondrial (*Acadm*, *Hmgcs2*)
328 (SI Fig. 6A). The transcripts for fatty acid transport were influenced in cPCLS by elafibranor,
329 as shown by the increased expression of *Fabp1*; for sPCLS only an increasing trend is
330 observed for this gene. However, the gene expression level of *Fabp1* in sPCLS was higher than
331 in cPCLS. The gene expression of *Scd1* and *Pdk4* were increased by elafibranor in both
332 groups, but the expression levels in sPCLS were lower than in cPCLS. Nonetheless, the fold
333 induction due to the treatment was higher in sPCLS compared to cPCLS. Additionally,
334 elafibranor 1 μM increased the expression of *Angptl4* and *Pex11a* only in cPCLS. No
335 differences were observed for the following genes: *Cd36*, *Me1*, *Apoa2*, *Apoa5* (SI Fig. 6A).
336 The effects of elafibranor were observed on transcriptional level of fat metabolism markers,
337 while no significant change was observed on the fibrosis area (SI Fig. 6B). These results show
338 that elafibranor can activate PPARα/δ signaling in murine PCLS, triggering the modulation of
339 lipid and carbohydrate metabolism, whereas fibrosis and inflammation were not affected in
340 PCLS during 48h culture.
341

342 **Elafibranor improves the metabolic profile and ameliorates fibrosis *in vivo* in CDAA diet**

343 We next asked if the results obtained with elafibranor *ex vivo* were predictive for *in vivo*. To
344 compare the results between the *ex vivo* and *in vivo* systems for the markers regulated by
345 PPARα/δ, Bl/6 mice were placed on the CDAA diet for 6 weeks, followed by 6 weeks of diet
346 and elafibranor treatment (15 mg/kg administered orally twice a day). Elafibranor improved
347 the metabolic profile with a reduction of liver triglycerides by 70% (Fig. 7A), but increased
348 liver weight compared to untreated mice (Fig. 7B). Regarding fibrosis, elafibranor reduced
349 total liver collagen (hyp) by 30% (Fig. 7C). In the same line, elafibranor reduced fibrosis
350 (*Col1a1*, *Acta2*) and inflammation (*Tnfa*) related transcripts (Fig. 7D). Treatment with
351 elafibranor beneficially modulated the transcripts of fat metabolism markers (Fig. 7E and SI
352 Fig. 7). After 6 weeks of treatment, elafibranor increased the mRNA expression of *Acox*, the
353 first enzyme involved in peroxisomal fatty acid β-oxidation. The drug also increased the gene
354 expression of enzymes involved in microsomal (*Cyp4a*) and mitochondrial (*Acadm*, *Hmgcs2*)
355 fatty acid oxidation. Elafibranor can increase fat metabolism in the liver by promoting: fatty
356 acid transport (*Cd36*, *Fabp1),* lipoprotein production *(Me1, Scd1),* trygliceride clearance
357 (*Angptl4*) and glucose metabolism inhibition (*Pdk4*). The gene expression of apolipoproteins
358 was differentially regulated by elafibranor, with *Apoa2* being increased and *Apoa5* being
359 decreased by the treatment. Lastly, elafibranor increased the expression of *Pex11a*, indicating
360 peroxisome proliferation.
361

Discussion

Our goal was to develop an *ex vivo* NASH model that closely mimics the changes associated with this condition and is relevant for testing therapeutic options. The model is based on steatotic murine livers as a source for PCLS, maintaining the original organ architecture and cellular composition.

The first part of the study focused on the viability of steatotic liver slices and the effects of culture. All slices remained viable, but for the overnutrition model (AMLN) we observed lower absolute values in ATP content compared to cPCLS, showing that steatosis etiology can influence PCLS viability. This difference might arise from the types of lipids accumulated in hepatocytes during NASH development in these livers. High carbohydrate and fructose feeding increases free fatty acids levels, especially due to *de novo* lipogenesis(49). The free fatty acids have a lipotoxic effect that leads to mitochondrial dysfunction(15), reduced ATP content and apoptosis via the death receptor Fas and TRAIL receptor 5(14, 35). Lack of choline was also associated with mitochondrial dysfunction(20), but the choline present in the culture media (14 μM) might have had a beneficial effect on CDAA slices, allowing them to recover and to have a similar ATP level to their cPCLS. The beneficial effect of choline in culture media (28 μM) was previously shown, when similar amounts of triacylglycerol were secreted by hepatocytes derived from mice on choline deficient and supplemented diets(28).

PCLS can be advantageous for NASH research, as culture spontaneously triggers key inflammation and fibrotic genes(33, 54). This could be beneficial especially for currently used *in vivo* steatotic murine models that show only mild inflammation and fibrosis. We expected an inflammatory and fibrotic response during incubation, together with higher gene expression levels in the sPCLS than cPCLS, since steatosis can trigger both inflammation(53) and fibrosis(40). Spontaneous fibrosis was observed in all PCLS during culture, with sPCLS surpassing cPCLS in regards to gene expression levels. Although the AMLN and CDAA diets induce steatosis through different mechanisms, the increase in fibrosis markers during culture was similar between the two diets. The results showed also a pro-inflammatory response

during culture in all PCLS; from the three analyzed markers, *Il6* was the most sensitive, having higher fold induction and attained expression levels in sPCLS. Increased levels of hepatic and circulating IL-6 were reported in animal models of NAFLD and patients(51, 68, 69). Long-term IL-6 stimulation aggravates NAFLD by inhibiting hepatic insulin receptor signaling, hence causing insulin resistance(48). Inflammation plays a role in NAFLD pathophysiology and prognosis; therefore, the pro-inflammatory effect induced by culture could help identify the roles of different cytokines and chemokines in NAFLD/NASH and their potential as therapeutic targets.

To our knowledge, this is the first study to assess gene expression related to lipid metabolism during culture of murine sPCLS. CDAA sPCLS showed less changes than AMLN sPCLS; this might be due to the decrease of fat metabolism related gene expression observed in the CDAA PCLS prior to culture (Fig. $2D_3$). The reduction of fat metabolism markers gene expression after culture can be caused by the absence of fructose, fatty acids and insulin in the culture media. Further investigations should be conducted to optimize the culture media in order to ensure the conservation and functionality of the lipid metabolism.

The versatility of the PCLS model is reflected by the possibility of enhancing biological processes in order to answer specific research questions. Therefore, in the second part of our study, we focused on further induction of inflammation and fibrosis to mimic *ex vivo* the pathology observed in NASH. This would allow mechanistic studies and drug testing in a variety of settings. For this reason, we tested if sPCLS can still respond to the effects of powerful modulators of inflammation (LPS) and fibrosis (TGFβ1), which are also associated with NASH in patients(6, 12, 34). The results showed that LPS can accentuate inflammation and the transcriptional levels reached were higher in steatotic slices than the controls. Interestingly, LPS activated PCLS from the AMLN model more intensively than CDAA diet. This could be caused by the presence of fructose in the AMLN, a nutrient that leads to the increased hepatic LPS levels and activation of toll-like receptor 4 signaling(50, 58). Although pre-exposure to LPS can lead to LPS tolerance(60), this can be different in NASH due to impaired LPS clearance and enhanced Kupffer cells activation(1). Additionally, the

composition of lipids stored in hepatocytes may modulate the activity of Kupffer cells(1). Marked inflammation could have a negative effect on fat catabolism, as the increased inflammation caused by LPS decreased the gene expression of the studied fat catabolism markers, especially in sPCLS.

Regarding fibrosis, TGFβ1 showed a clear profibrotic effect. sPCLS reached higher expression levels for fibrosis markers than cPCLS, confirming that we can accentuate fibrosis *ex vivo*, especially in the presence of steatosis and fibrosis. This is in accordance with human data, where an overexpression of the *TGFB1* gene was found in NASH patients with fibrosis compared to NASH patients without fibrosis(5). An interesting result was that TGFβ1 could increase the production of pro-collagen Iα1 only in healthy slices. The lack of response from sPCLS could be due to the fact that a maximum production of pro-collagen Iα1 is induced solely by culture. Moreover, the high secretion of this protein in sPCLS when compared to cPCLS could be explained by more ECM-secreting cells in steatotic slices and a more susceptible response to the profibrotic effect of culture. Additionally, TGFβ1 reduced the gene expression of fat metabolism markers, especially for sPCLS, showing that an ongoing fibrotic process may contribute to lipid metabolism compromise. The detrimental effect of TGFβ1 in NAFLD was reported in murine hepatocytes, where TGFβ1 had a synergistic effect on palmitate, increasing lipogenesis and decreasing catabolism markers(70). Altogether, we showed that sPCLS are still responsive to further induction of fibrosis or inflammation, processes that also impact fat metabolism. This shows that the model is not limited to the effects triggered by culture and we can accentuate pathological conditions with activators or inhibitors, generating various stages of disease.

Development and efficacy assessment of drugs is an expensive and time-consuming process. More relevant *in vitro* methods are needed to prevent unnecessary *in vivo* animal studies. Therefore, the goal of the last part of this study was to determine if the *ex vivo* steatotic PCLS model could be used for testing anti-NAFLD compounds. An advantage of this model is that several compounds and concentrations can be studied in slices from the same animal. We chose to evaluate the effects of elafibranor, since it is a promising candidate for treating

445 NASH, with good results in clinical trials(44). In addition, we aimed to investigate if this drug
446 had a direct effect on fibrosis and inflammation in PCLS, since elafibranor can reduce
447 inflammation and fibrosis in mice *in vivo*(59). Elafibranor activates lipid catabolism as a result
448 of PPARα/δ activation. Transcriptional markers of fatty acid oxidation were increased by
449 elafibranor in healthy control and CDAA sPCLS and in our *in vivo* experiment; however, the
450 gene expression of mitochondrial oxidation markers was induced only *in vivo*. This may
451 indicate that mitochondrial oxidation needs more than 48h (PCLS incubation time) to be
452 induced by elafibranor, while the activation of PPARα triggers initial microsomal and
453 peroxisomal oxidation. Elafibranor had similar effects in PCLS and *in vivo* for fatty acid
454 transport transcripts, where it increased *Fabp1* expression. FABP1, has an antioxidant and
455 detoxifying role(64, 65) in hepatocytes due to its function in intracellular storage and transport
456 of fatty acids. Moreover, a reduced level of FABP1 was reported in NASH patients and might
457 predict NASH susceptibility in NAFLD patients(9). By increasing *Fabp1* gene expression,
458 elafibranor shows a protective role against oxidative stress and NAFLD progression. Another
459 positive effect of elafibranor on lipid metabolism regulation was the increase of *Scd1* gene
460 expression, which was achieved in PCLS and *in vivo*. This gene was reported to be
461 downregulated in animal models of NAFLD(16) and the hepatic protein activity was
462 negatively correlated with liver fat in obese patients(52). Moreover, elafibranor influences
463 glucose metabolism by inducing *Pdk4*, *ex vivo* as well as *in vivo*. Increased *Pdk4* expression
464 shows that glucose metabolism is inhibited and fatty acids are used instead to provide energy
465 for the cell(46). A characteristic effect of PPARα agonists in the liver of rodents is hepatocyte
466 peroxisome proliferation, which causes liver enlargement through hyperplasia and
467 hypertrophy(2). Interestingly, the activation of PPARα in man does not lead to cell
468 proliferation and therefore, the agonists of this receptor do not have a hepatocarcinogenic
469 potential(57). Peroxisome proliferation in rodents was reported *in vivo* and *in vitro*(2). This
470 process was observed in our study from the increased gene expression of *Pex11a (ex vivo* and
471 *in vivo)* and liver weight increase *in vivo*. These results might indicate that the efficacy of
472 elafibranor in increasing fat oxidation in mice is achieved through peroxisome proliferation. *Ex*

473 *vivo*, elafibranor showed clear effects on promoting fatty acids catabolism, but it does not
474 ameliorate fibrosis and inflammation. *In vivo*, six weeks of elafibranor treatment had positive
475 effects on fibrosis, inflammation and fat metabolism. We believe that in the *in vivo*
476 experiments elafibranor improved lipid metabolism due to its mechanism of action, whereas
477 amelioration of fibrosis and inflammation are indirect effects due to the reduction of fat and
478 oxidative stress. Since fibrosis is triggered by inflammation, a reduction of inflammation
479 would have a beneficial effect on fibrosis. The effects on inflammation and fibrosis are not
480 observed in sPCLS probably due to the short culture time, but the similar effects on genes
481 modulated by PPARα/δ are a confirmation that PCLS can correctly predict the efficacy of a
482 drug on certain targets (receptors/pathways). Mouse results cannot be directly translated to
483 patients, especially since the two species show different sensitivity to peroxisome proliferation,
484 which might indicate faster steatosis resolution in mice than humans. Nevertheless, the phase
485 two clinical trial of elafibranor showed that after one year, NASH patients had substantial
486 histological improvement and resolution of steatohepatitis, without fibrosis worsening(44).
487 Given these points, we consider that PCLS might have high predictive value for evaluating the
488 efficacy of anti-NAFLD compounds.
489 An important aspect of animal experiments is the relevance for human disease. NAFLD has a
490 complex and heterogeneous pathogenesis, characterized by numerous interrelated processes
491 that occur in different organs (liver, intestine, adipose tissue)(4). Although the methods used to
492 induce NAFLD in animals are derived from human studies (overnutrition, diets rich in fat and
493 carbohydrates, choline deprivation), the animal models of NAFLD may not recapitulate all
494 characteristics of the condition(13). The overnutrition models show similar metabolic features
495 to patients; however, the outcome is not severe and requires more time to develop(23). The
496 choline deficient diet needs less time to show steatohepatitis features and fibrosis similar to
497 patients with rapid NASH progression(26). However, in CDAA-fed mice the metabolic profile
498 is opposite to the human condition, as they do not gain body weight, nor do they display
499 hepatic insulin resistance(19). The animal model choice for preparing sPCLS depends mostly
500 on the scientific question that needs to be answered. The chosen animal model for obtaining

PCLS should take into consideration the drug's mechanism of action. The overnutrition model of AMLN can elucidate questions regarding steatosis, while CDAA is more indicated for later NAFLD stages, where increased inflammation and fibrosis can be investigated. We consider both models relevant for preclinical drug development, as they displayed increased inflammation and fibrosis during culture, and responded to pro-inflammatory and profibrotic stimuli. Additionally, modulators of inflammation and fibrosis can create more severe phenotypes to inquire drug efficacy. The model cannot replace *in vivo* experiments, but can reduce the number of animals by providing more relevant outcomes regarding safety and efficacy.

Based on our data, we suggest that sPCLS is a promising tool to study NASH pathogenesis and test pharmaceutical compounds. Beside murine PCLS, this model could be used for (fatty) human livers from surgical procedures, in order to exclude murine-human translation. Nevertheless, there are drawbacks of the PCLS model, such as absence of communication with other organs involved in NAFLD, such as adipose tissue, or circulating immune cells and adipokines. However, it is still possible to study the effect of the adipose tissue on liver *in vitro*, by co-culturing sPCLS with adipocytes. Another option is the addition of adipokines to the sPCLS incubation media. An alternative to sPCLS would be inducing fat accumulation *in vitro* in healthy murine/human PCLS by adding fatty acids, sugars and insulin to the culture media(41). Although we observed that the transcripts of fat metabolism related markers are decreased during PCLS incubation, this might change in the presence of fatty acids, as observed *in vitro* in hepatocytes(39). Therefore, we consider that murine steatotic PCLS are fundamental for paving the way for studies in human liver slices (culture conditions optimization).

In conclusion, PCLS appear to be a valuable preclinical model that preserves liver cellular structure and reduces significantly the number of animals used for research. Steatotic PCLS can be obtained from various animal models with different degrees of steatosis and fibrosis. As an *ex vivo* model, sPCLS shows fibrosis, inflammation and fat metabolism transcriptional changes during culture. Fibrosis and inflammation can be further induced with specific

529 molecules and drugs can be evaluated for their anti-NAFLD effect. The selection of the animal
530 model should be done according to the research question. Future studies should be conducted
531 to optimize culture conditions, especially for the lipid metabolism, and to obtain the proof of
532 clinical translation of new NAFLD therapies, as a critical step for sPCLS validation.
533

Acknowledgments:

This study was supported by ZonMw (the Netherlands Organisation for Health Research and Development) – grant number 114025003.

DS receives project related support by the EU Horizon 2020 under grant agreement n. 634413 (EPoS, European Project on Steatohepatitis) and 777377 (LITMUS, Liver Investigation on Marker Utility in Steatohepatitis), and by the German Research Foundation collaborative research project grants DFG CRC 1066/B3 and CRC 1292/08.

We would like to thank Anke Voigt (Boehringer Ingelheim) for excellent technical support with *in vivo* experiments.

Author contributions

EG designed the experiments in collaboration with PO and MB. AB provided the murine tissue for experiments. EG, EB, and AO performed the experiments, processed the experimental data and performed the analysis. EG designed the figures. EG wrote the manuscript with critical review from EB, AO, DS, MB, JFR, AB. and PO. All authors discussed the results and contributed to the final manuscript.

Conflict of interest:

A. Oldenburger, J.F. Rippmann and A. Broermann are employees at Boehringer Ingelheim Pharma GmbH & Co. KG.

References

1. **Baffy G**. Kupffer cells in non-alcoholic fatty liver disease: The emerging view. *J Hepatol* 51: 212–223, 2009.
2. **Bentley P**, **Calder I**, **Elcombe C**, **Grasso P**, **Stringer D**, **Wiegand HJ**. Hepatic peroxisome proliferation in rodents and its significance for humans. *Food Chem Toxicol* 31: 857–907, 1993.
3. **Bojic LA**, **Sawyez CG**, **Telford DE**, **Edwards JY**, **Hegele RA**, **Huff MW**. Activation of peroxisome proliferator-activated receptor δ inhibits human macrophage foam cell formation and the inflammatory response induced by very low-density lipoprotein. *Arterioscler Thromb Vasc Biol* 32: 2919–2928, 2012.
4. **Byrne CD**, **Targher G**. Review NAFLD : A multisystem disease. *J Hepatol* 62: S47–S64, 2015.
5. **Cayón A**, **Crespo J**, **Mayorga M**, **Guerra A**, **Pons-Romero F**. Increased expression of Ob-Rb and its relationship with the overexpression of TGF- b 1 and the stage of fibrosis in patients with nonalcoholic steatohepatitis. *Liver Int* : 1065–1071, 2006.
6. **Ceccarelli S**, **Panera N**, **Mina M**, **Gnani D**, **De Stefanis C**, **Crudele A**, **Rychlicki C**, **Petrini S**, **Bruscalupi G**, **Agostinelli L**, **Stronati L**, **Cucchiara S**, **Musso G**, **Furlanello C**, **Svegliati-Baroni G**, **Nobili V**, **Alisi A**. LPS-induced TNF-a factor mediates pro-inflammatory and pro-fibrogenic pattern in non-alcoholic fatty liver disease. *Oncotarget* 6, 2015.
7. **Chalasani N**, **Younossi Z**, **Lavine JE**, **Charlton M**, **Cusi K**, **Rinella M**, **Harrison SA**, **Brunt EM**, **Sanyal AJ**. The diagnosis and management of nonalcoholic fatty liver disease: Practice guidance from the American Association for the Study of Liver Diseases. *Hepatology* 67: 328–357, 2018.
8. **Charlton M**, **Krishnan A**, **Viker K**, **Sanderson S**, **Cazanave S**, **McConico A**, **Masuoko H**, **Gores G**. Fast food diet mouse: novel small animal model of NASH with ballooning, progressive fibrosis, and high physiological fidelity to the human condition. *AJP Gastrointest Liver Physiol* 301: G825–G834, 2011.
9. **Charlton M**, **Viker K**, **Krishnan A**, **Sanderson S**, **Kaalsbeek AJ**, **Kendrick M**, **Thompson G**, **Que F**, **Sarr M**. Differential Expression of Lumican and Fatty Acid Binding Protein-1 – New Insights into the Histologic Spectrum of Non- Alcoholic Fatty Liver Disease. *Hepatology* 49: 1375–1384, 2009.
10. **Clapper JR**, **Hendricks MD**, **Gu G**, **Wittmer C**, **Dolman CS**, **Herich J**, **Athanacio J**, **Villescaz C**, **Ghosh SS**, **Heilig JS**, **Lowe C**, **Roth JD**. Diet-induced mouse model of fatty liver disease and nonalcoholic steatohepatitis reflecting clinical disease progression and methods of assessment. *Am J Physiol Liver Physiol* 305: G483–G495, 2013.
11. **Desvergne B**, **Wahli W**. Peroxisome Proliferator-Activated Receptors: Nuclear Control of Metabolism. *Endocr Rev* 20: 649–688, 1999.
12. **Farhadi A**, **Gundlapalli S**, **Shaikh M**, **Frantzides C**, **Harrell L**, **Kwasny MM**, **Keshavarzian A**. Susceptibility to gut leakiness: a possible mechanism for endotoxaemia in non-alcoholic steatohepatitis. *Liver Int* 28: 1026–1033, 2008.
13. **Farrell G**, **Schattenberg JM**, **Leclercq I**, **Yeh MM**, **Goldin R**, **Teoh N**, **Schuppan D**. Mouse models of nonalcoholic steatohepatitis Towards optimization of their relevance to human NASH. *Hepatology* 2: 0–2, 2018.
14. **Feldstein AE**, **Canbay A**, **Guicciardi ME**, **Higuchi H**, **Bronk SF**, **Gores GJ**.

Diet associated hepatic steatosis sensitizes to Fas mediated liver injury in mice. *J Hepatol* 39: 978–983, 2003.

15. **Feldstein AE**, **Werneburg NW**, **Canbay A**, **Guicciardi ME**, **Bronk SF**, **Rydzewski R**, **Burgart LJ**, **Gores GJ**. Free fatty acids promote hepatic lipotoxicity by stimulating TNF-?? expression via a lysosomal pathway. *Hepatology* 40: 185–194, 2004.
16. **Fernández Gianotti T**, **Burgueño A**, **Gonzales Mansilla N**, **Pirola CJ**, **Sookoian S**. Fatty Liver Is Associated with Transcriptional Downregulation of Stearoyl-CoA Desaturase and Impaired Protein Dimerization. *PLoS One* 8: 1–11, 2013.
17. **Fukunishi S**, **Sujishi T**, **Takeshita A**, **Ohama H**, **Tsuchimoto Y**, **Asai A**, **Tsuda Y**, **Higuchi K**. Lipopolysaccharides accelerate hepatic steatosis in the development of nonalcoholic fatty liver disease in Zucker rats. *J Clin Biochem Nutr* 54: 39–44, 2014.
18. **de Graaf IAM**, **Olinga P**, **de Jager MH**, **Merema MT**, **de Kanter R**, **van de Kerkhof EG**, **Groothuis GMM**. Preparation and incubation of precision-cut liver and intestinal slices for application in drug metabolism and toxicity studies. *Nat Protoc* 5: 1540–1551, 2010.
19. **Hebbard L**, **George J**. Animal models of nonalcoholic fatty liver disease [Online]. *Nat Rev Gastroenterol &Amp; Hepatol* 8: 35, 2010. https://doi.org/10.1038/nrgastro.2010.191.
20. **Hensley K**. Dietary choline restriction causes complex I dysfunction and increased H2O2 generation in liver mitochondria. *Carcinogenesis* 21: 983–989, 2000.
21. **Van Herck M**, **Vonghia L**, **Francque S**. Animal Models of Nonalcoholic Fatty Liver Disease—A Starter's Guide. *Nutrients* 9: 1072, 2017.
22. **Ijssennagger N**, **Janssen AWF**, **Milona A**, **Ramos Pittol JM**, **Hollman DAA**, **Mokry M**, **Betzel B**, **Berends FJ**, **Janssen IM**, **Van Mil SWC**, **Kersten S**. Gene expression profiling in human precision cut liver slices in response to the FXR agonist obeticholic acid. *J Hepatol* 64: 1158–1166, 2016.
23. **Ito M**, **Suzuki J**, **Tsujioka S**, **Sasaki M**, **Gomori A**, **Shirakura T**, **Hirose H**, **Ito M**, **Ishihara A**, **Iwaasa H**, **Kanatani A**. Longitudinal analysis of murine steatohepatitis model induced by chronic exposure to high-fat diet. *Hepatol Res* 37: 50–57, 2007.
24. **Kalia HS**, **Gaglio PJ**. The Prevalence and Pathobiology of Nonalcoholic Fatty Liver Disease in Patients of Different Races or Ethnicities. *Clin Liver Dis* 20: 215–224, 2016.
25. **Kodama Y**, **Kisseleva T**, **Iwaisako K**, **Miura K**, **Taura K**, **De S**. NIH Public Access. *October* 137: 1467–1477, 2010.
26. **Kodama Y**, **Kisseleva T**, **Iwaisako K**, **Miura K**, **Taura K**, **De Minicis S**, **Österreicher CH**, **Schnabl B**, **Seki E**, **Brenner DA**. c-Jun N-terminal Kinase-1 From Hematopoietic Cells Mediates Progression From Hepatic Steatosis to Steatohepatitis and Fibrosis in Mice. *Gastroenterology* 137: 1467-1477.e5, 2009.
27. **Kohli R**, **Kirby M**, **Xanthakos SA**, **Softic S**, **Feldstein AE**, **Tang PH**, **Miles L**, **Miles M V**, **Balistreri WF**, **Stephen C**, **Seeley RJ**. High-Fructose Medium-Chain-Trans-Fat Diet Induces Liver Fibrosis & Elevates Plasma Coenzyme Q9 in a Novel Murine Model of Obesity and NASH. *Hepatology* 52: 934–944, 2010.
28. **Kulinski A**, **Vance DE**, **Vance JE**. A Choline-deficient Diet in Mice Inhibits

neither the CDP-choline Pathway for Phosphatidylcholine Synthesis in Hepatocytes nor Apolipoprotein B Secretion. *J Biol Chem* 279: 23916–23924, 2004.

29. **Lau JKC**, **Zhang X**, **Yu J**. Animal models of non-alcoholic fatty liver disease: current perspectives and recent advances. *J Pathol* 241: 36–44, 2017.
30. **Li Z**, **Agellon LB**, **Vance DE**. Phosphatidylcholine homeostasis and liver failure. *J Biol Chem* 280: 37798–37802, 2005.
31. **Liu Z-M**, **Hu M**, **Chan P**, **Tomlinson B**. Early investigational drugs targeting PPAR-α for the treatment of metabolic disease. *Expert Opin Investig Drugs* 24: 611–621, 2015.
32. **Longato L**. Non-alcoholic fatty liver disease (NAFLD): a tale of fat and sugar? *Fibrogenesis Tissue Repair* 6: 14, 2013.
33. **Luangmonkong T**, **Suriguga S**, **Bigaeva E**, **Boersema M**, **Oosterhuis D**, **de Jong KP**, **Schuppan D**, **Mutsaers HAM**, **Olinga P**. Evaluating the antifibrotic potency of galunisertib in a human ex vivo model of liver fibrosis. *Br J Pharmacol* 174: 3107–3117, 2017.
34. **Mahmoud AA**, **Bakir AS**, **Shabana SS**. Serum TGF-β, Serum MMP-1, and HOMA-IR as non-invasive predictors of fibrosis in Egyptian patients with NAFLD. *Saudi J Gastroenterol* 18: 327–33, 2012.
35. **Malhi H**, **Barreyro FJ**, **Isomoto H**, **Bronk SF**, **Gores GJ**. Free fatty acids sensitise hepatocytes to TRAIL mediated cytotoxicity. *Gut* 56: 1124–1131, 2007.
36. **Mandard S**, **Müller M**, **Kersten S**. Peroxisome proliferator-activated receptor a target genes. *Cell Mol Life Sci* 61: 393–416, 2004.
37. **Meng XM**, **Nikolic-Paterson DJ**, **Lan HY**. TGF-β: The master regulator of fibrosis. *Nat Rev Nephrol* 12: 325–338, 2016.
38. **Noga AA**, **Vance DE**. A gender-specific role for phosphatidylethanolamine N-methyltransferase-derived phosphatidylcholine in the regulation of plasma high density and very low density lipoproteins in mice. *J Biol Chem* 278: 21851–21859, 2003.
39. **Park MJ**, **Kim D Il**, **Choi JH**, **Heo YR**, **Park SH**. New role of irisin in hepatocytes: The protective effect of hepatic steatosis in vitro. *Cell Signal* 27: 1831–1839, 2015.
40. **Peverill W**, **Powell LW**, **Skoien R**. Evolving concepts in the pathogenesis of NASH: Beyond steatosis and inflammation. *Int J Mol Sci* 15: 8591–8638, 2014.
41. **Prins G**, **Luangmonkong T**, **Oosterhuis D**, **Mutsaers H**, **Dekker F**, **Olinga P**. A Pathophysiological Model of Non-Alcoholic Fatty Liver Disease Using Precision-Cut Liver Slices. *Nutrients* 11: 507, 2019.
42. **Qi C**, **Zhu Y**, **Reddy JK**. Peroxisome Proliferator-Activated Receptors, Coactivators, and Downstream Targets. *Cell Biochem Biophys* 32: 187–204, 2000.
43. **Rakhshandehroo M**, **Knoch B**, **Müller M**, **Kersten S**. Peroxisome Proliferator-Activated Receptor Alpha Target Genes. *PPAR Res* 2010: 1–20, 2010.
44. **Ratziu V**, **Harrison SA**, **Francque S**, **Bedossa P**, **Lehert P**, **Serfaty L**, **Romero-Gomez M**, **Boursier J**, **Abdelmalek M**, **Caldwell S**, **Drenth J**, **Anstee QM**, **Hum D**, **Hanf R**, **Roudot A**, **Megnien S**, **Staels B**, **Sanyal A**, **Mathurin P**, **Gournay J**, **Nguyen-Khac E**, **De Ledinghen V**, **Larrey D**, **Tran A**, **Bourliere M**, **Maynard-Muet M**, **Asselah T**, **Henrion J**, **Nevens F**, **Cassiman D**, **Geerts A**, **Moreno C**, **Beuers UH**, **Galle PR**, **Spengler U**,

Bugianesi E, **Craxi A**, **Angelico M**, **Fargion S**, **Voiculescu M**, **Gheorghe L**, **Preotescu L**, **Caballeria J**, **Andrade RJ**, **Crespo J**, **Callera JL**, **Ala A**, **Aithal G**, **Abouda G**, **Luketic V**, **Huang MA**, **Gordon S**, **Pockros P**, **Poordad F**, **Shores N**, **Moehlen MW**, **Bambha K**, **Clark V**, **Satapathy S**, **Parekh S**, **Reddy RK**, **Sheikh MY**, **Szabo G**, **Vierling J**, **Foster T**, **Umpierrez G**, **Chang C**, **Box T**, **Gallegos-Orozco J**. Elafibranor, an Agonist of the Peroxisome Proliferator−Activated Receptor−α and −δ, Induces Resolution of Nonalcoholic Steatohepatitis Without Fibrosis Worsening. *Gastroenterology* 150: 1147-1159.e5, 2016.

45. **Rotman Y**, **Sanyal AJ**. Current and upcoming pharmacotherapy for non-alcoholic fatty liver disease. *Gut* 66: 180–190, 2017.

46. **Savkur RS**, **Bramlett KS**, **Michael LF**, **Burris TP**. Regulation of pyruvate dehydrogenase kinase expression by the farnesoid X receptor. *Biochem Biophys Res Commun* 329: 391–396, 2005.

47. **Schuppan D**, **Surabattula R**, **Wang XY**. Determinants of fibrosis progression and regression in NASH. *J Hepatol* 68: 238–250, 2018.

48. **Senn JJ**, **Klover PJ**, **Nowak IA**, **Zimmers TA**, **Koniaris LG**, **Furlanetto RW**, **Mooney RA**. Suppressor of Cytokine Signaling-3 (SOCS-3), a Potential Mediator of Interleukin-6-dependent Insulin Resistance in Hepatocytes *. 278: 13740–13746, 2003.

49. **Softic S**, **Cohen DE**, **Kahn CR**. Role of Dietary Fructose and Hepatic De Novo Lipogenesis in Fatty Liver Disease. *Dig Dis Sci* 61: 1282–1293, 2016.

50. **Spruss A**, **Kanuri G**, **Wagnerberger S**, **Haub S**, **Bischoff SC**, **Bergheim I**. Toll-like receptor 4 is involved in the development of fructose-induced hepatic steatosis in mice. *Hepatology* 50: 1094–1104, 2009.

51. **Steatohepatitis N**, **Se B**, **Mas E**, **Danjoux M**, **Garcia V**. IL-6 Deficiency Attenuates Murine Diet-Induced. 4: 1–10, 2009.

52. **Stefan N**, **Peter A**, **Cegan A**, **Staiger H**, **Machann J**, **Schick F**, **Claussen CD**, **Fritsche A**, **Häring HU**, **Schleicher E**. Low hepatic stearoyl-CoA desaturase 1 activity is associated with fatty liver and insulin resistance in obese humans. *Diabetologia* 51: 648–656, 2008.

53. **Stojsavljević S**, **Gomerčić Palčić M**, **Jukić, Virović L**, **Smirčić Duvnjak L**, **Duvnjak M**. Adipokines and proinflammatory cytokines, the key mediators in the pathogenesis of nonalcoholic fatty liver disease. *World J Gastroenterol* 20: 18070–18091, 2014.

54. **Stribos EGD**, **Luangmonkong T**, **Leliveld AM**, **de Jong IJ**, **van Son WJ**, **Hillebrands J-L**, **Seelen MA**, **van Goor H**, **Olinga P**, **Mutsaers HAM**. Precision-cut human kidney slices as a model to elucidate the process of renal fibrosis. *Transl Res* 170: 8-16.e1, 2016.

55. **Stribos EGD**, **Seelen MA**, **van Goor H**, **Olinga P**, **Mutsaers HAM**. Murine Precision-Cut Kidney Slices as an ex vivo Model to Evaluate the Role of Transforming Growth Factor-β1 Signaling in the Onset of Renal Fibrosis. *Front Physiol* 8: 1–9, 2017.

56. **Suriguga S**, **Luangmonkong T**, **Bigaeva E**, **Oosterhuis D**, **Mutsaers HAM**, **Groothuis GMM**, **Olinga P**. LPS aggravates fibrosis only in the early onset but not in the end stage of liver fibrosis. *Hepatology* 64: 840A, 2016.

57. **Thomas M**, **Bayha C**, **Klein K**, **Müller S**, **Weiss TS**, **Schwab M**, **Zanger UM**. The truncated splice variant of peroxisome proliferator-activated receptor alpha, PPARα-tr, autonomously regulates proliferative and pro-inflammatory genes. *BMC Cancer* 15: 488, 2015.

58. **Thuy S**, **Ladurner R**, **Volynets V**, **Wagner S**, **Strahl S**, **Königsrainer A**, **Maier K-P**, **Bischoff SC**, **Bergheim I**. Nonalcoholic Fatty Liver Disease in Humans Is Associated with Increased Plasma Endotoxin and Plasminogen Activator Inhibitor 1 Concentrations and with Fructose Intake. *J Nutr* 138: 1452–1455, 2008.
59. **Tølbøl KS**, **Kristiansen MNB**, **Hansen HH**, **Veidal SS**, **Rigbolt KTG**, **Gillum MP**, **Jelsing J**, **Vrang N**, **Feigh M**. Metabolic and hepatic effects of liraglutide, obeticholic acid and elafibranor in diet-induced obese mouse models of biopsy-confirmed nonalcoholic steatohepatitis. *World J Gastroenterol* 24: 179–194, 2018.
60. **Uhrig A**, **Banafsche R**, **Kremer M**, **Hegenbarth S**, **Hamann A**, **Neurath M**, **Gerken G**, **Limmer A**, **Knolle PA**. Development and functional consequences of LPS tolerance in sinusoidal endothelial cells of the liver thelial cells (LSEC) clear portal venous blood from TLR4 surface expression of LSEC is not altered by Isolation of murine LSEC. (2005). doi: 10.1189/jlb.0604332.
61. **Vatakuti S**, **Pennings JLA**, **Gore E**, **Olinga P**, **Groothuis GMM**. Classification of Cholestatic and Necrotic Hepatotoxicants Using Transcriptomics on Human Precision-Cut Liver Slices. *Chem Res Toxicol* 29, 2016.
62. **de Waal Malefyt R**. Interleukin 10(IL-10) inhibits cytokine synthesis by human monocytes: an autoregulatory role of IL-10 produced by monocytes. *J Exp Med* 174: 1209–1220, 1991.
63. **Walczak R**, **Carole B**, **Benoit N**, **Descamps E**, **Nathalie D**, **Megnien S**, **Hum D**, **Staels B**, **Friedman S**, **Loomba R**, **Harrison S**. Elafibranor and nitazoxanide synergize to reduce fibrosis in a NASH model. *J Hepatol* 68: S352–S353, 2018.
64. **Wang G**, **Gong Y**, **Anderson J**, **Sun D**, **Minuk G**, **Roberts MS**, **Burczynski FJ**. Antioxidative function of L-FABP in L-FABP stably transfected Chang liver cells. *Hepatology* 42: 871–879, 2005.
65. **Wanninger J**, **Neumeier M**, **Hellerbrand C**, **Schacherer D**, **Bauer S**, **Weiss TS**, **Huber H**, **Schäffler A**, **Aslanidis C**, **Schölmerich J**, **Buechler C**. Lipid accumulation impairs adiponectin-mediated induction of activin A by increasing TGFbeta in primary human hepatocytes. *Biochim Biophys Acta - Mol Cell Biol Lipids* 1811: 626–633, 2011.
66. **Westra IM**, **Mutsaers HAM**, **Luangmonkong T**, **Hadi M**, **Oosterhuis D**, **de Jong KP**, **Groothuis GMM**, **Olinga P**. Human precision-cut liver slices as a model to test antifibrotic drugs in the early onset of liver fibrosis. *Toxicol Vitr* 35: 77–85, 2016.
67. **Westra IM**, **Pham BT**, **Groothuis GMM**, **Olinga P**. Evaluation of fibrosis in precision-cut tissue slices. *Xenobiotica* 43: 98–112, 2013.
68. **Wieckowska A**, **Papouchado BG**, **Li Z**, **Lopez R**, **Zein NN**, **Feldstein AE**. Liver and Biliary Tract Increased Hepatic and Circulating Interleukin-6 Levels in Human Nonalcoholic Steatohepatitis. 6: 1372–1379, 2008.
69. **Yamaguchi K**, **Itoh Y**, **Yokomizo C**, **Nishimura T**, **Niimi T**, **Fujii H**, **Okanoue T**, **Yoshikawa T**. Blockade of interleukin-6 signaling enhances hepatic steatosis but improves liver injury in methionine choline-deficient diet-fed mice. *Lab Investig* 90: 1169–1178, 2010.
70. **Yang L**, **Roh YS**, **Song J**, **Zhang B**, **Liu C**, **Loomba R**, **Seki E**. Transforming growth factor beta signaling in hepatocytes participates in steatohepatitis through regulation of cell death and lipid metabolism in mice. *Hepatology* 59:

483–495, 2014.

71. **Younossi Z**, **Anstee QM**, **Marietti M**, **Hardy T**, **Henry L**, **Eslam M**, **George J**, **Bugianesi E**. Global burden of NAFLD and NASH: trends, predictions, risk factors and prevention. *Nat Rev Gastroenterol Hepatol* 15: 11–20, 2017.

Figure legends

Fig. 1 – Schematic representation of the NAFLD induction in Bl/6 mice and precision-cut liver preparation and culture.

Fig. 2 – The effects of AMLN and CDAA on the livers of Bl/6 mice. (**A**) Liver to body weight ratio; (**B**) Hydroxyproline (hyp) content; (**C**) H&E and Sirius Red staining of representative mouse liver section; Note the presence of macrosteatosis (black arrow), microsteatosis (white arrow), inflammatory infiltrated cells (dashed arrow), ballooning degeneration (double head black arrow) and collagen I and III fibers (black arrow head); (**D**) mRNA expression levels of (**D1**) fibrosis, (**D2**) inflammation and (**D3**) fat metabolism related markers in PCLS prior culture. *p*-value assessed by Mann-Whitney test ; **p* < 0.05, ***p*<0.01, ****p*<0.001 significantly different from livers of the corresponding control diet. Data are expressed as means (± SEM), n=4 for AMLN, n=3 for hyp AMLN, n=4 for CTR AMLN, n=10 for CDAA diet and n=8 for CTR CDAA diet.

Fig. 3 – The effects of 48h culture on PCLS regarding (A) fibrosis, (B) inflammation and (C) fat metabolism related markers. mRNA expression levels of markers after 48h culture; fold induction is relative to cPCLS prior culture, using the corresponding control diet for each NAFLD-inducing diet; Data are expressed as means (± SEM); *p*-value assessed by Mann-Whitney test; **p* < 0.05, ***p*<0.01, ****p*<0.001 significantly different from PCLS of the corresponding diet prior incubation (0h); n=4 for AMLN and CTR AMLN, n=10 for CDAA diet and n=8 for CTR CDAA .

Fig. 4 – The effects of LPS on PCLS regarding (A) fibrosis markers, (B) pro-collagen Iα1 secretion, (C) inflammation and (D) fat metabolism related markers. mRNA expression levels of markers after 48h LPS treatment; fold induction is relative to cPCLS prior culture (0h), using the corresponding control diet for each NAFLD-inducing diet; Pro-collagen Iα1 released in the culture media in the last 24h of incubation of control and steatotics PCLS treated with LPS; Data are expressed as means (± SEM); *p*-value assessed by Mann-Whitney test; **p* < 0.05, ***p*<0.01, ****p*<0.001 significantly different from PCLS of the corresponding diet; n=4 for AMLN and CTR AMLN, n=10 for CDAA diet, n=8 for CTR CDAA diet, n=5 for pro-collagen Iα1 CDAA and CTR CDAA.

Fig. 5 – The effects of TGFβ1 on PCLS regarding (A) fibrosis markers, (B) pro-collagen Iα1 secretion, (C) inflammation and (D) fat metabolism related markers. mRNA expression levels of markers after 48h TGFβ1 treatment; fold induction is relative to cPCLS prior culture (0h), using the corresponding control diet for each NAFLD-inducing diet; Pro-collagen Iα1 released in the culture media in the last 24h of incubation of control and steatotics PCLS treated with TGFβ1; Data are expressed as means (± SEM); *p*-value assessed by Mann-Whitney test; **p* < 0.05, ***p*<0.01, ****p*<0.001 significantly different from PCLS of the corresponding diet; n=4 for AMLN, n=3 for CTR AMLN, n=9 for CDAA, n=8 for CTR CDAA, pro-collagen Iα1: n=5 for CDAA and CTR CDAA and n=4 for AMLN and CTR AMLN. .

Fig. 6 – The effect of elafibranor in steatotic and control CDAA PCLS. mRNA expression levels of (**A**) fibrosis, (**B**) inflammation, (**C**) fat metabolism related markers after 48h elafibranor treatment (0.2 or 1 μM); fold induction is relative to cPCLS prior culture (0h); Data are expressed as means (± SEM); *p*-value assessed by Kruskal-Wallis test (exact *p* value); **p* < 0.05, ***p*<0.01, ****p*<0.001 significantly different from untreated PCLS of the corresponding diet; n=4 for CTR CDAA and n=5 for CDAA PCLS.

Fig. 7 – The effect of elafibranor on mice on CDAA diet. (**A**) Serum triglycerides; (**B**) Liver to body weight ratios; (**C**) Hepatic hyp content expressed as µg hyp/mg liver tissue; mRNA expression levels of (**D**) fibrosis, inflammation, and (**E**) fat metabolism related markers; fold induction is relative to mice on CDAA treated with vehicle; Data are expressed as means (± SEM), *p*-value assessed by Mann-Whitney test; **p* < 0.05, ***p*<0.01, ****p*<0.001 significantly different from CDAA vehicle; n=11.

Supplementary figures

S1 –Masson's trichrome staining of representative mouse liver sections from mice on AMLN and CDAA and their corresponding control diets.
Supplemental Material available at
URL: https://figshare.com/s/19c5e641d85460ee0b20
DOI: 10.6084/m9.figshare.11310515

S2 – The mRNA expression levels of fibrosis, inflammation and fat metabolism markers in mouse PCLS obtained from mice on the control diets for AMLN and CDAA diets.
Supplemental Material available at
URL: https://figshare.com/s/3d60c81eeb44731879f7
DOI: 10.6084/m9.figshare.8966267

S3 – Viability of murine PCLS from mice on AMLN and CDAA and their corresponding control diets.
Supplemental Material available at
URL: https://figshare.com/s/460965ae3d8f30d95da1
DOI: 10.6084/m9.figshare.8966327

S4 - The effect of TGFβ1 on the fibrotic area of AMLN and CDAA sPCLS and cPCLS.
Supplemental Material available at
URL: https://figshare.com/s/04dc920a89b309cdc54a
DOI: 10.6084/m9.figshare.8966330

S5 - The effect of CDAA diet on fat metabolism in murine livers.
Supplemental Material available at
URL: https://figshare.com/s/628e714cc0b605875371
DOI: 10.6084/m9.figshare.8966333

S6 - The effect of elafibranor *ex vivo* in CDAA s/cPCLS.
Supplemental Material available at
URL: https://figshare.com/s/e77fc1cd8dec825531c5
DOI: 10.6084/m9.figshare.8966336

S7 - The effect of elafibranor *in vivo* in CDAA-fed mice.
Supplemental Material available at
URL: https://figshare.com/s/23f5c930b9409ff68c15
DOI: 10.6084/m9.figshare.8966339

Table 1 – Overview of Sybr Green primers

Name	Forward	Reverse
Hmbs	ATGAGGGTGATTCGAGTGGG	TTGTCTCCCGTGGTGGACATA
Col1a1	TGACTGGAAGAGCGGCGAGT	ATCCATCGGTCATGCTCTCT
Serpinh1	AGGTCACCAAGGATGTGGAG	CAGCTTCTCCTTCTCGTCGT
Acta2	ACTACTGCCGAGCGTGAGAT	CCAATGAAAGATGGCTGGAA
Fn1	CGGAGAGAGTGCCCCTACTA	CGATATTGGTGAATCGCAGA
Il1b	GCCAAGACAGGTCGCTCAGGG	CCCCCACACGTTGACAGCTAGG
Il6	TGATGCTGGTGACAACCACGGC	TAAGCCTCCGACTTGTGAAGTGGTA
Tnf	CTGTAGCCCACGTCGTAGC	TTGAGATCCATGCCGTTG
Fasn	CTGCGGAAACTTCAGGAAATG	GGTTCGGAATGCTATCCAGG
Acaca	GCGTCGGGTAGATCCAGTT	CTCAGTGGGGCTTAGCTCTG
Acox	ATGCCTTTGTTGTCCCTATC	CCATCTTCAGGTAGCCATTATC
Cpt1a	TCCACCCTGAGGCATCTATT	ATGACCTCCTGGCATTCTCC
Ppara	CACGCATGTGAAGGCTGTAA	GCTCCGATCACACTTGTCG
Cyp4a	GCTAGCTCCTTGGATTGGGTA	AGGGTTTCAGAATGTCATAGTGG
Acadm	AGTACCCTGTGGAGAAGCTGAT	TCAATGTGCTCACGAGCTATG
Hmgcs2	CTGTGGCAATGCTGATCG	TCCATGTGAGTTCCCCTCA
Cd36	TTGAAAAGTCTCGGACATTGAG	TCAGATCCGAACACAGCGTA
Fabp1	CCATGACTGGGGAAAAAGTC	GCCTTTGAAAGTTGTCACCAT
Me1	CAGAGGCCCTGAGTATGACG	CCGATTGGCAAAATCTTCAA
Scd1	TTCCCTCCTGCAAGCTCTAC	CAGAGCGCTGGTCATGTAGT
Apoa2	CAGCACAGAATCGCACTGTT	TCCGTCTGCCTGTCTCTTAAC
Apoa5	GCCAAAACAGTTGGAGCAA	GAAGCTGCCTTTCAGGTTCTC
Angptl4	GGGACCTTAACTGTGCCAAG	GAATGGCTACAGGTACCAAACC
Pdk4	CGCTTAGTGAACACTCCTTCG	CTTCTGGGCTCTTCTCATGG
Pex11a	TTCATCCGAGTCGCCAAC	CATGCATGCGTGCTGAGT

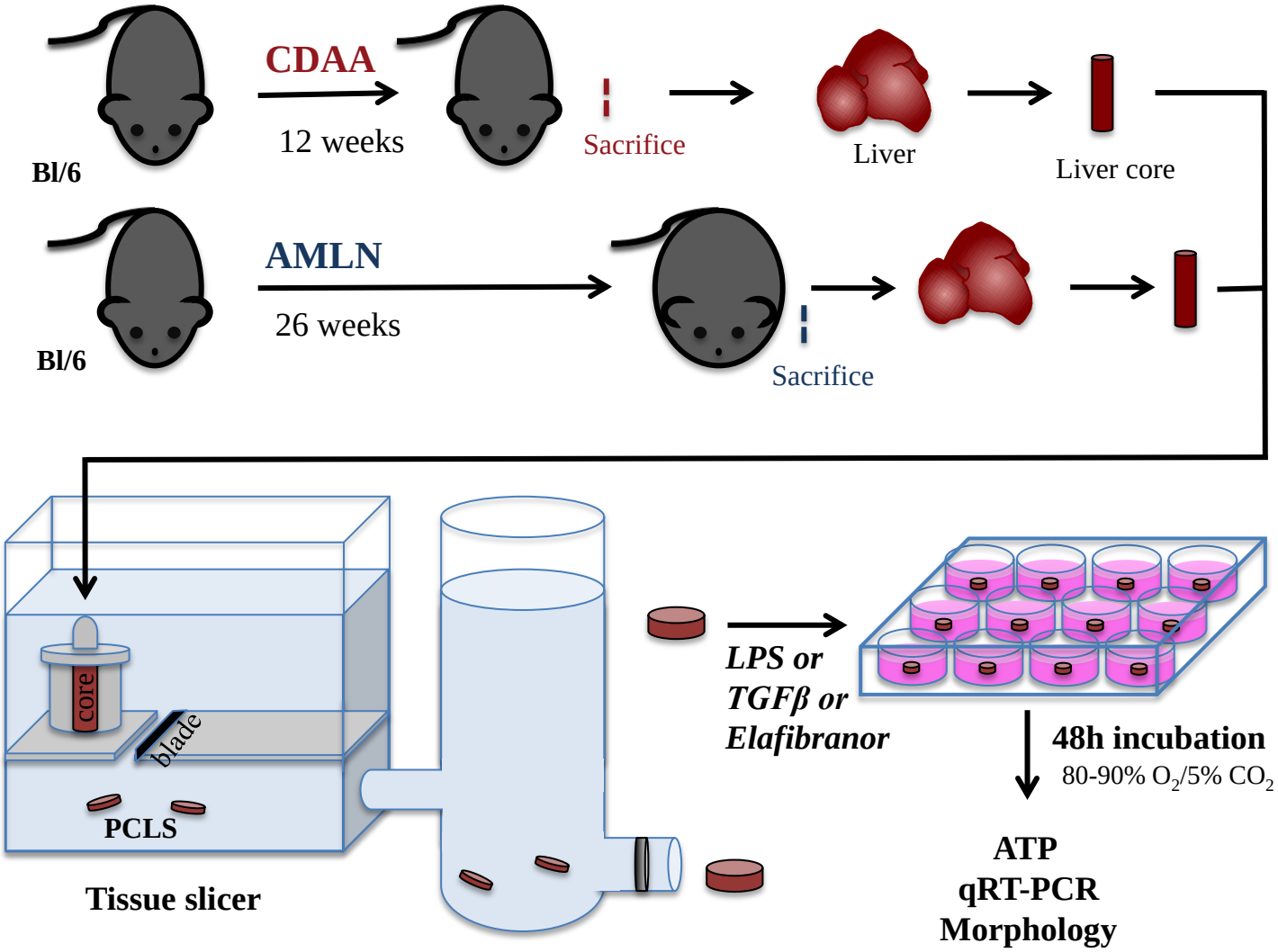

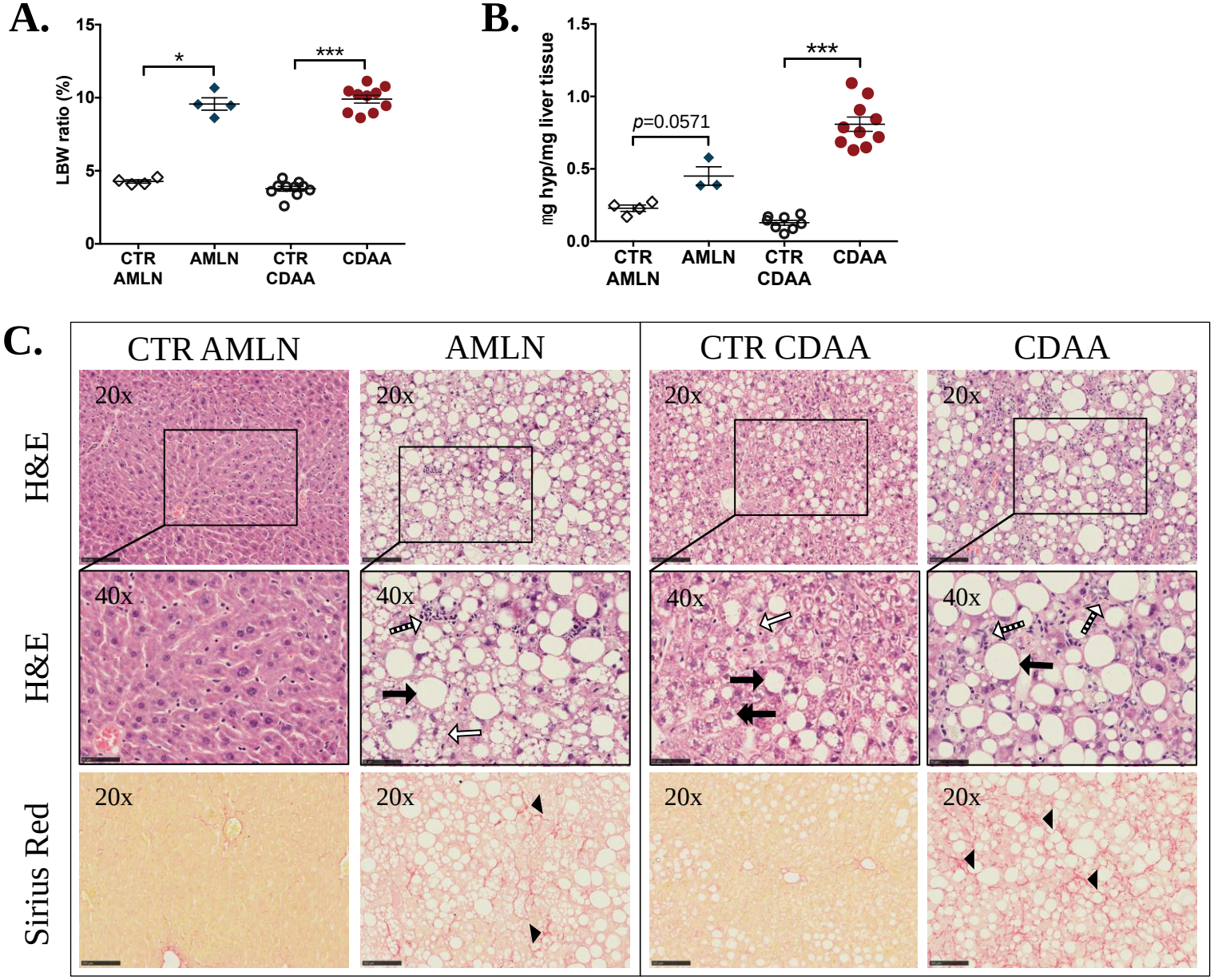

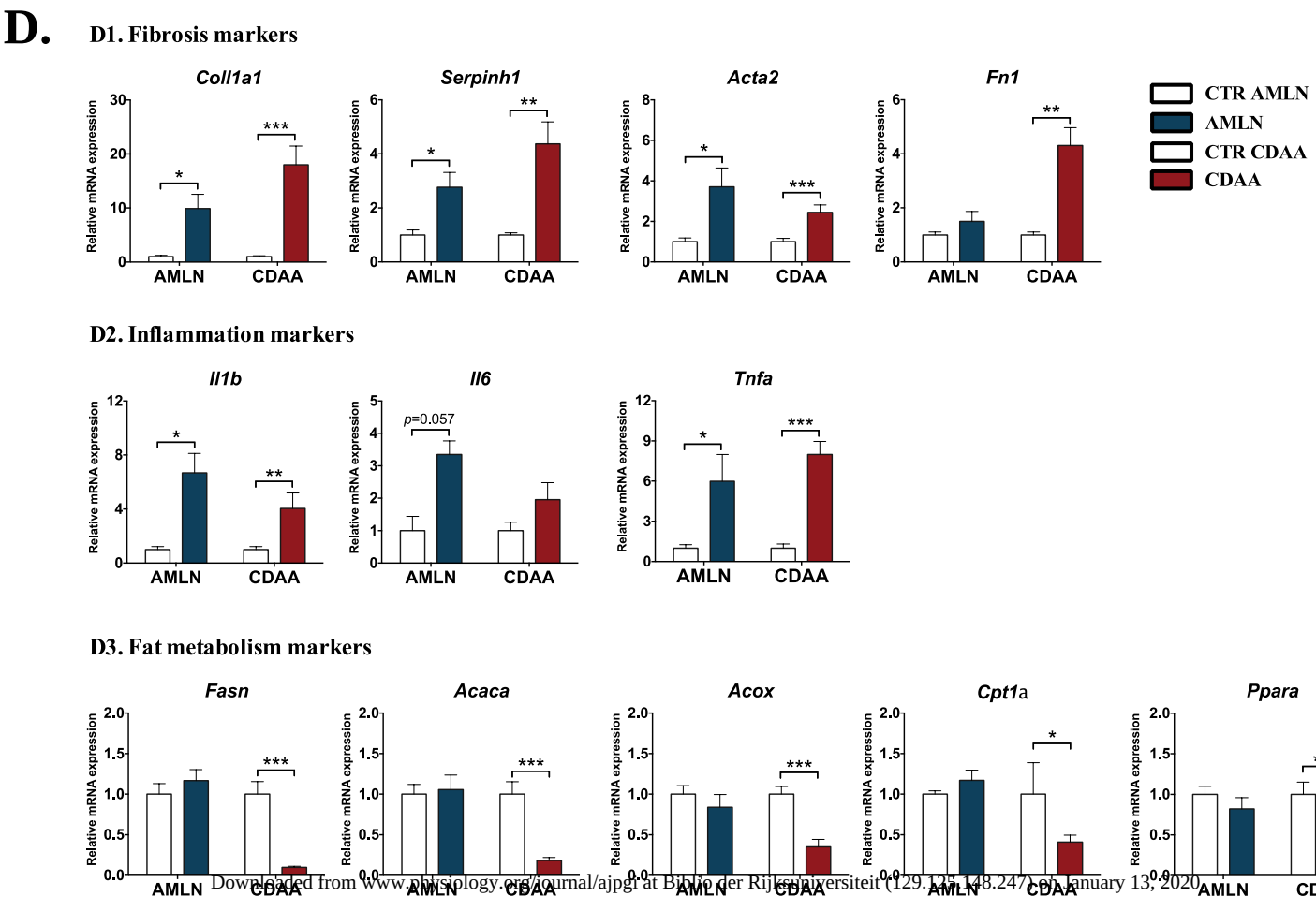

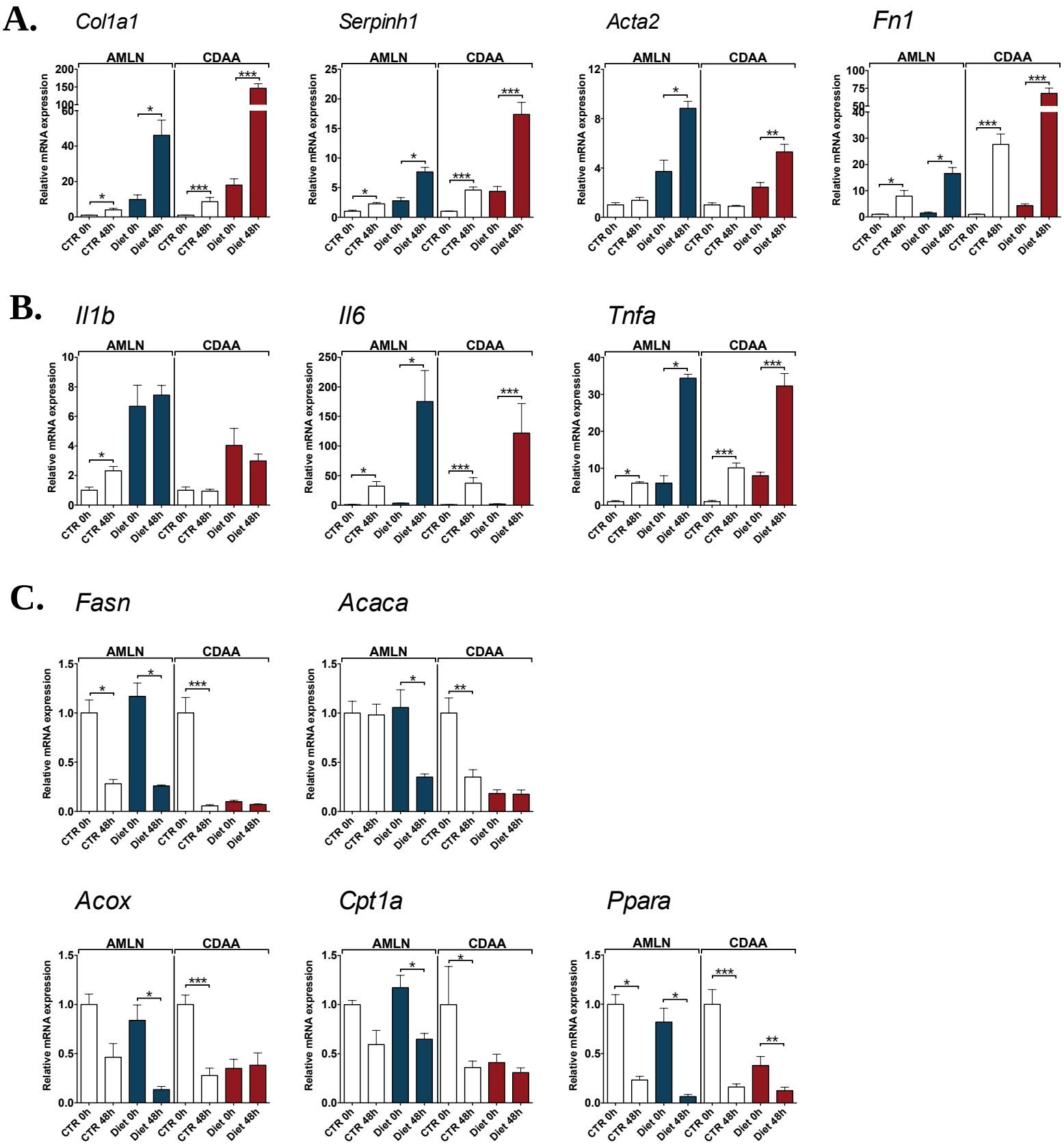

A. *Col1a1*

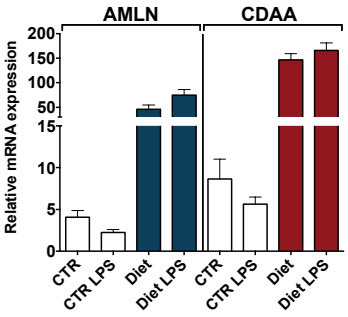

Serpinh1

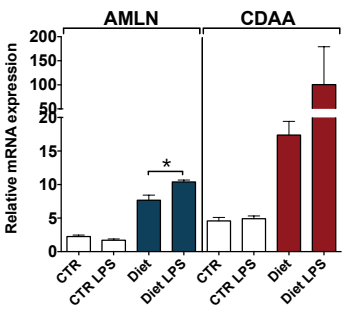

Acta2

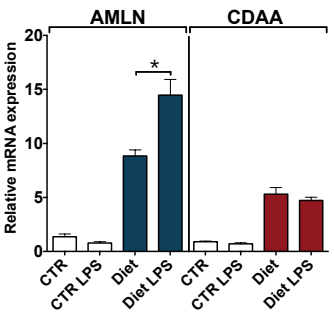

Fn1

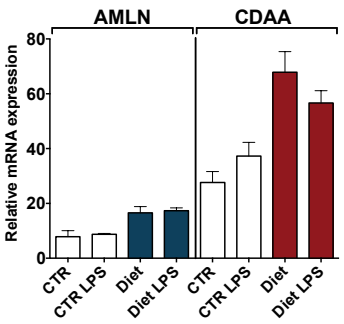

B. Pro-collagen Ia1

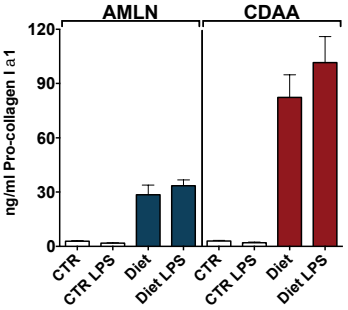

C. *Il1b*

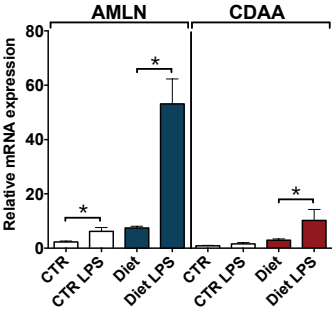

Il6

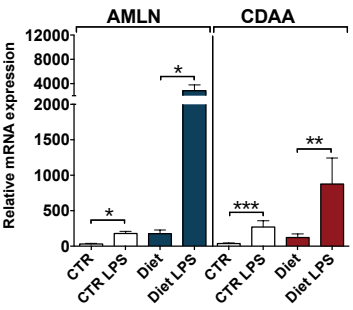

Tnfa

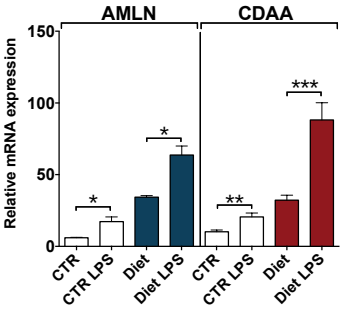

D. *Fasn*

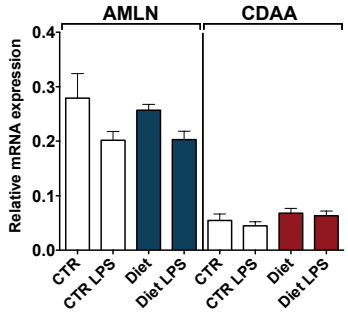

Acaca

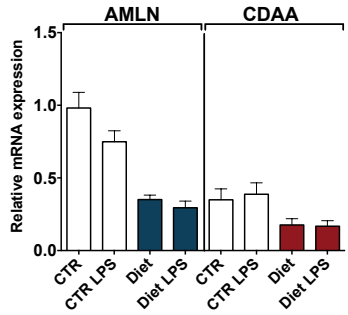

Acox

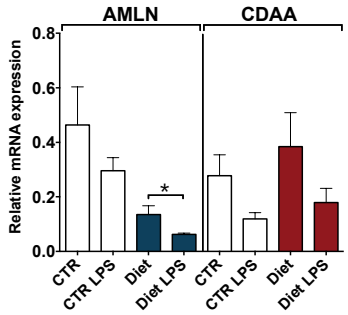

Cpt1a

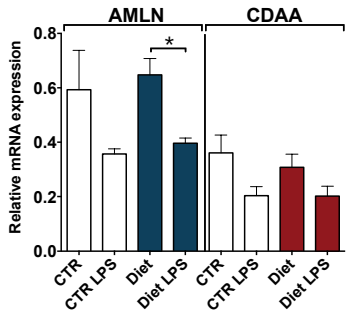

Ppara

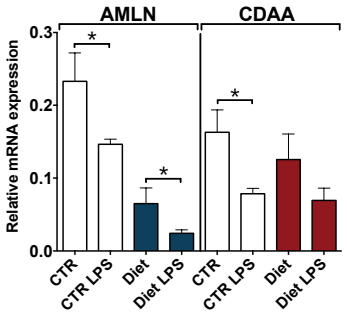

A. *Col1a1*

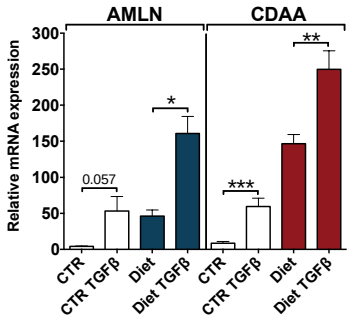

Serpinh1

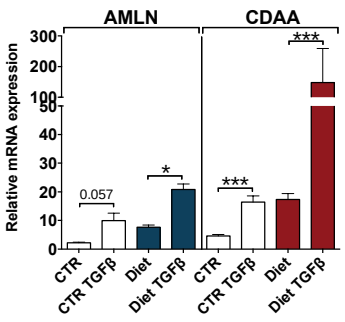

Acta2

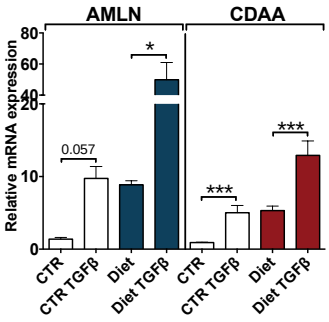

Fn1

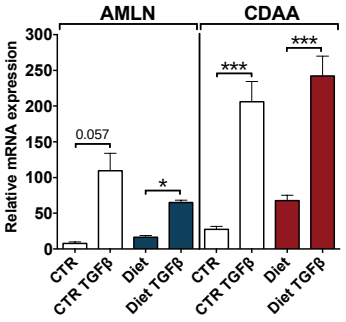

B. Pro-collagen Ia1

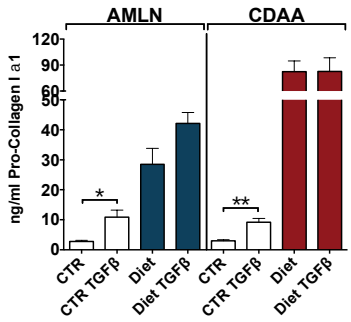

C. *Il1b*

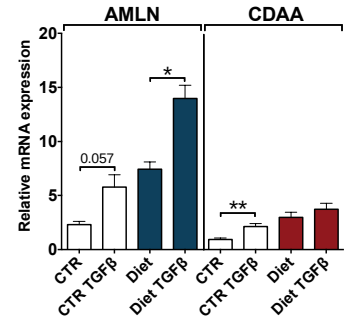

Il6

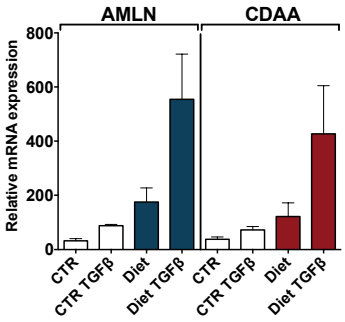

Tnfa

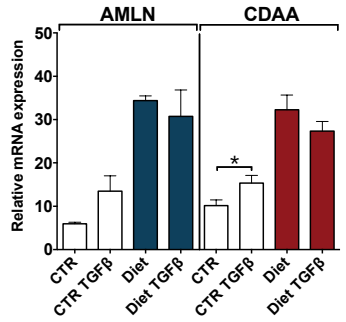

D. *Fasn*

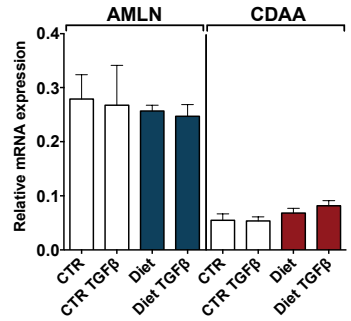

Acaca

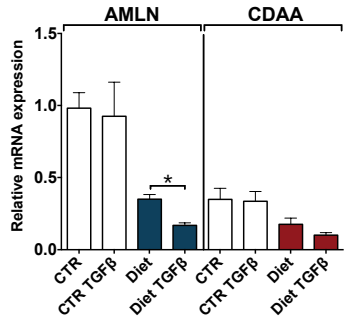

Acox

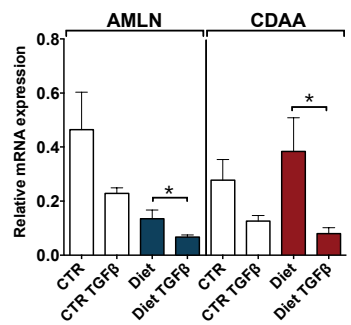

Cpt1a

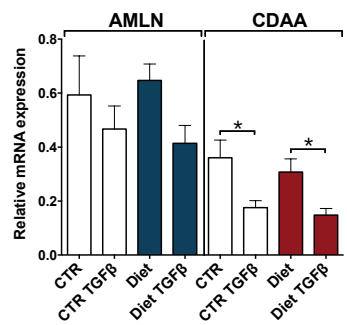

Ppara

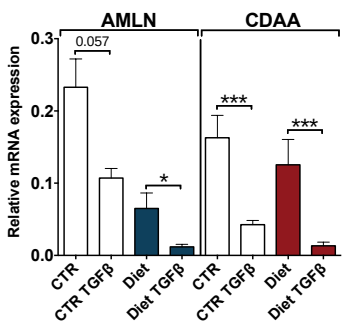

A.

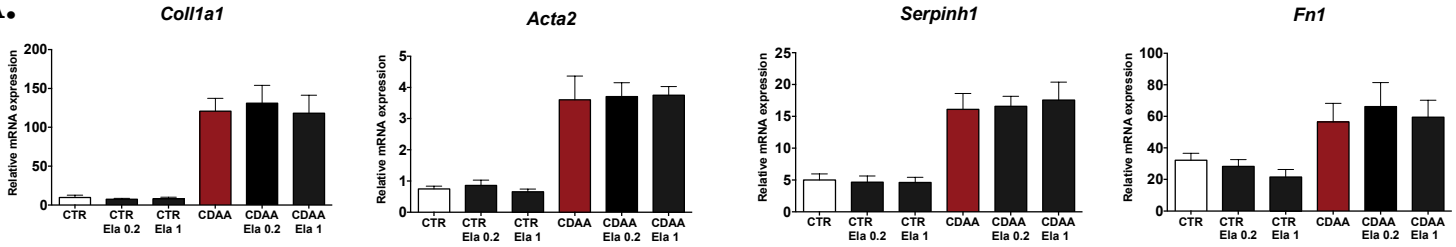

B.

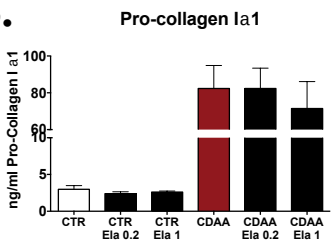

C.

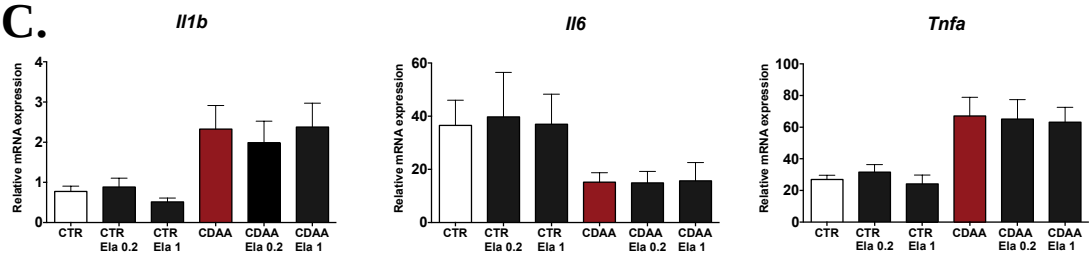

D.

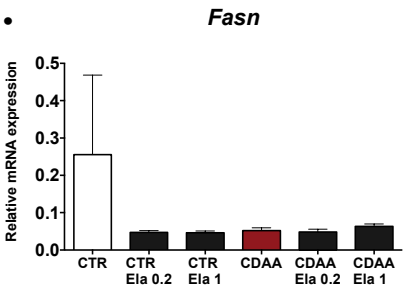

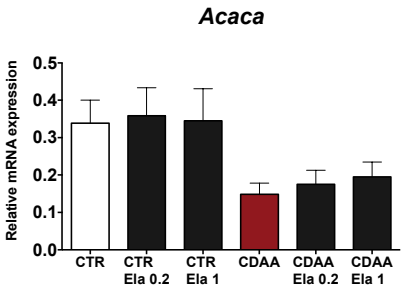

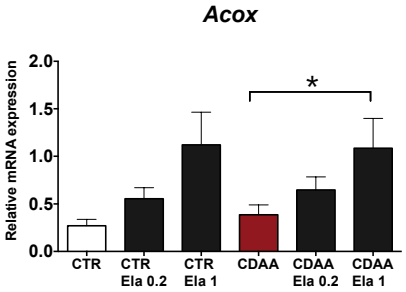

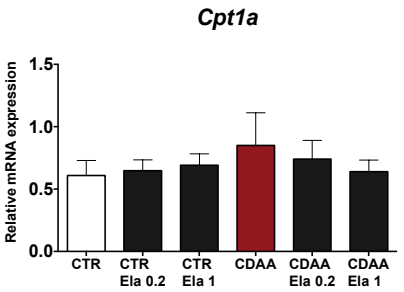

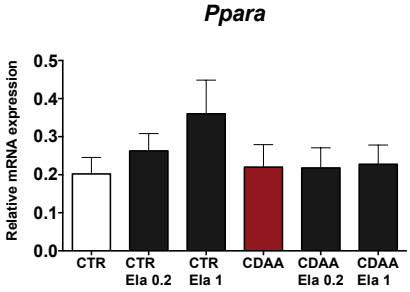

Fatty acid oxidation and ketogenesis

Fatty acid and very low density lipoproteins production

Fatty acid transport

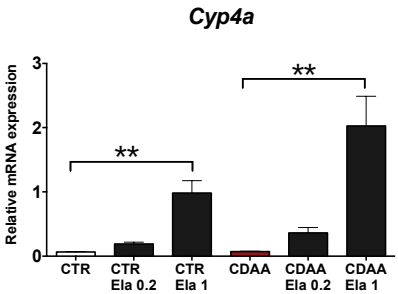

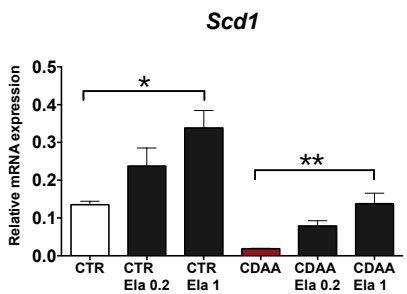

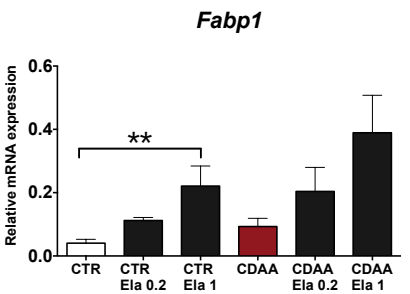

Triglyceride clearance

Glucose metabolism

Peroxizome proliferation

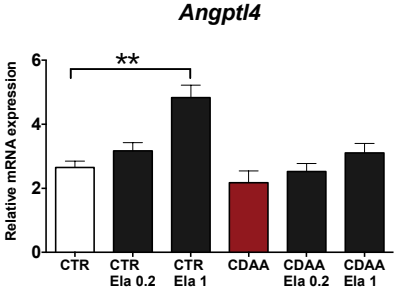

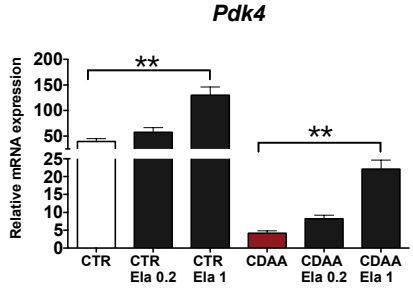

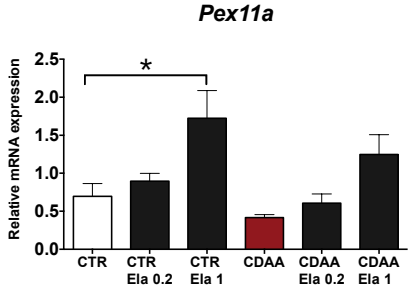

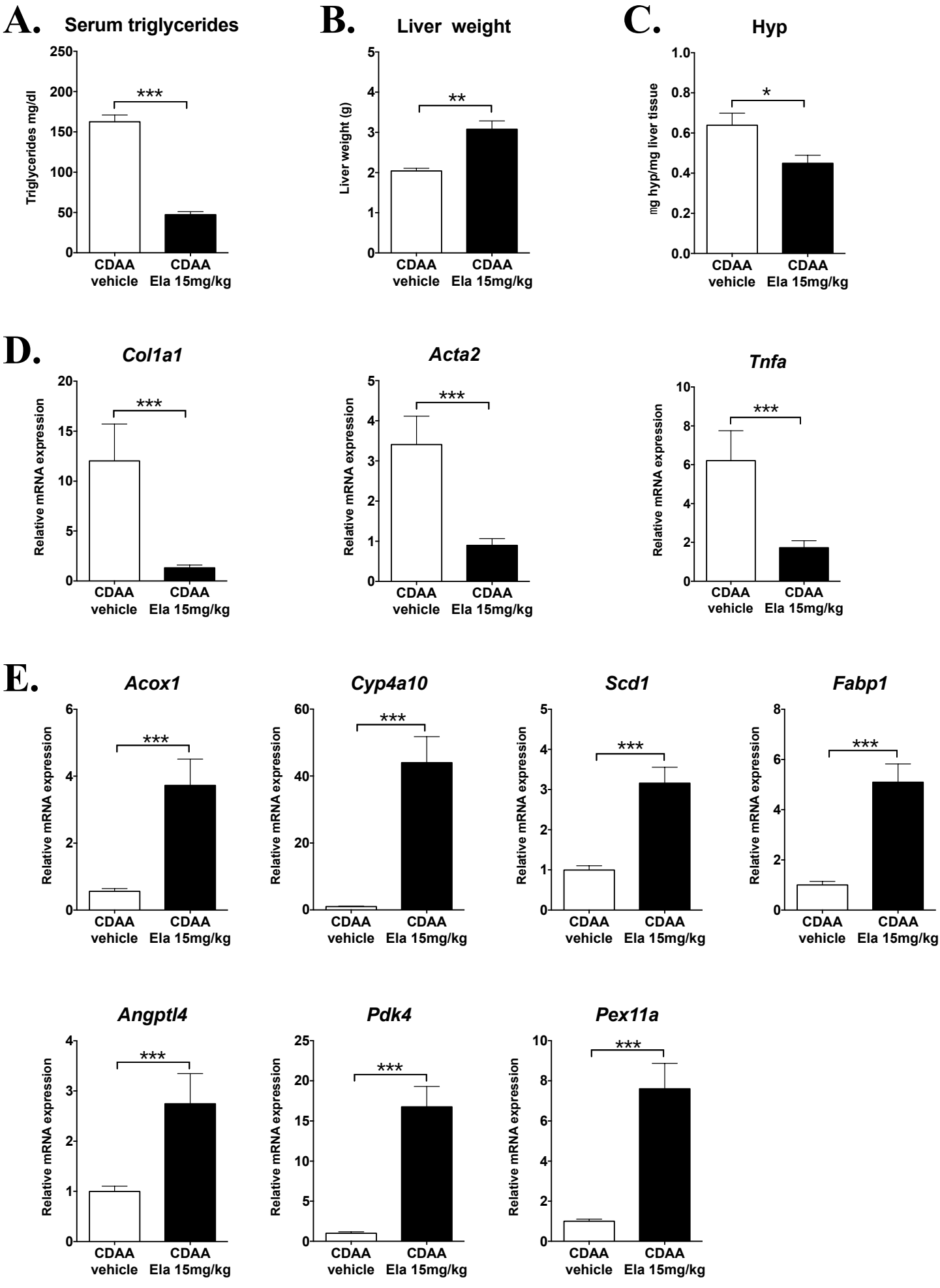

A. *Ex vivo*

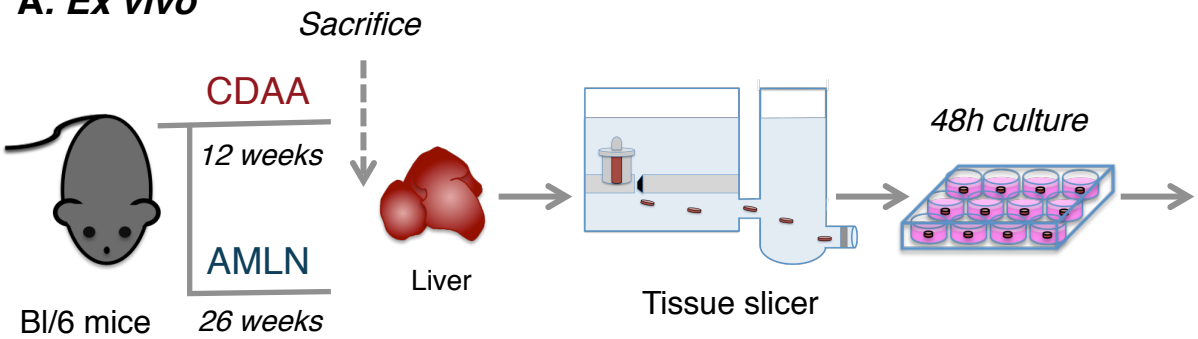

	Fibrosis	Inflammation	Lipid metabolism
Control	↑	↑	↓
LPS	-	↑↑	-
TGFβ	↑↑	-	↓
Elafibranor	-	-	↑

B. *In vivo*

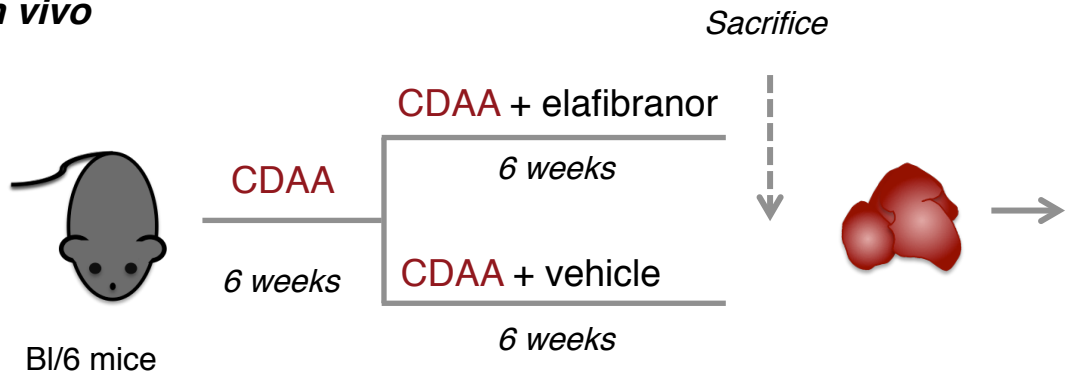

	Fibrosis	Inflammation	Lipid metabolism
Elafibranor	↓	↓	↑